JOURNAL OF GUIDANCE, CONTROL, AND DYNAMICS
Vol. 24, No. 5, September–October 2001

Nonlinear Regulation for Tracking and Drag Compensation of Two-Body Spinning Satellite

P. Di Giamberardino,* S. Monaco,† and R. Ronchini‡
University of Rome "La Sapienza," 00184 Rome, Italy

A nonlinear controller is designed for achieving low-orbit stabilization and asymptotic rejection of the atmospheric drag of a two-body spinning satellite. The choice of the mechanical structure and the use of low-power actuators are inspired by a scientific mission under study: Galileo Galilei, a small mission for a high-precision test of the equivalence principle. The feasibility of the proposed controller and its robustness are confirmed by the results of some simulations.

Nomenclature

$\mathbb{C}^-$	=	strictly negative complex half-plane
c_t, c_f, c_r	=	damping coefficients (translational and rotational) of a spring
d	=	drag force
$\tilde{E}_{AD}$	=	area of active damper (AD) thrust over 200 s of steady state
$\hat{E}_{AD}$	=	area of AD thrust over 200 s of transient
$\tilde{E}_{FEEP}$	=	area of field emission electric propulsion (FEEP) thrust over 200 s of steady state
$\hat{E}_{FEEP}$	=	area of FEEP thrust over 200 s of transient
e	=	subscript referring to the external body
G_u	=	universal gravitational constant
i	=	subscript referring to the inner body
$J_{p\,PGB}$	=	principal inertial momentum of picogravity box (PGB)
$J_{p\,S/C}$	=	principal inertial momentum of spacecraft S/C
$J_{p\,TM_e}$	=	principal inertial momentum of external test mass (TM)
$J_{p\,TM_i}$	=	principal inertial momentum of internal TM
J_t, J_p	=	inertial momentums of cylinder in the mathematical model
$J_{t\,PGB}$	=	transversal inertial momentum of PGB
$J_{t\,S/C}$	=	transversal inertial momentum of S/C
$J_{t\,TM_e}$	=	transversal inertial momentum of external TM
$J_{t\,TM_i}$	=	transversal inertial momentum of internal TM
k_t, k_f, k_r	=	elastic coefficients (translational and rotational) of a spring
$\mathcal{L}$	=	Lagrange function
m	=	mass of the cylinder in the mathematical model
m_{PGB}	=	mass of PGB
$m_{S/C}$	=	mass of S/C
m_{TM_e}	=	mass of external TM
m_{TM_i}	=	mass of internal TM
$m_\oplus$	=	Earth mass
$\mathcal{Q}$	=	generalized forces
$\mathcal{T}$	=	kinetic energy
$\tilde{T}_{AD}$	=	maximum steady-state AD thrust
T^*_{AD}	=	maximum active dampers thrust
$\tilde{T}_{FEEP}$	=	maximum steady-state FEEP thrust
T^*_{FEEP}	=	maximum FEEP thrust
$t_{0.1}$	=	time necessary to reach 10% of the initial value of the response
$\mathcal{U}$	=	potential energy
Γ	=	vector of gravity center in the inertial reference frame, (x, y, z)
$\Delta\tilde{c}$	=	steady-state relative displacement of gravity centers
Δc^*	=	maximum relative displacement of gravity centers
δ	=	center of masses misalignment, $(\epsilon_x, \epsilon_y, \epsilon_z)$
$\tilde{\theta}$	=	spin angle in standard form
$\sigma(A)$	=	spectrum of matrix A
Φ	=	vector of Euler angles, (ϕ, ψ, θ)
χ	=	couple unbalance
Ω	=	angular velocity in body frame
ω	=	angular velocity in inertial frame
$\omega_o/2\pi$	=	orbital frequency
$\omega_s/2\pi$	=	spin frequency

Introduction

THE number of spacecraft orbiting around the Earth has been greatly increasing in recent years. A number of missions in modern space applications make use of low-Earth orbit (LEO) satellites. For a LEO satellite, the atmospheric drag represents a not negligible periodic perturbation of uncertain amplitude. Thus, roughly speaking, the orbit control problem can be formulated in terms of tracking a periodic trajectory against the action of an uncertain periodic perturbation.

The paper shows that a natural setting for studying such a control problem is the nonlinear regulation technique developed in Ref. 1. Such an approach is here developed with reference to Galileo Galilei,[2–4] a spacecraft to support an Italian high-precision scientific mission, currently under study, designed to test the equivalence principle (EP) to 1 part in 10^{17}, an improvement of five orders of magnitude over the best results obtained thus far. The satellite evolves on a LEO orbit at the altitude of about 520 km. It is composed of four concentric hollow rigid cylinders, weakly coupled by means of soft springs, spinning around their symmetry axis at the supercritical frequency of 2 Hz; active dampers (AD), that is, electrostatic actuators, act between these cylinders. The outer cylinder is the spacecraft shell. Inside the so-called picogravity box (PGB), the second cylinder contains two coaxial cylindrical test masses (TMs) coupled by damped soft springs with a read-out capacitance plates among them for accurate sensing of their relative displacements. The external actuators are constituted by field emission electric propulsion (FEEP)[5] thrusters, low-power thrusters that can supply modulable continuous forces. An EP violation should produce a tiny displacement of the two inner masses measured by the capacitive sensors.

Because the main problem addressed in the paper refers to the orbit keeping against the drag forces acting on the spacecraft, the two inner masses can be neglected. As a consequence, throughout the paper, we will refer to a simplified mechanical structure constituted by two nested cylinders, the external one representing the spacecraft (S/C) and the internal one representing the PGB. This

Received 15 October 1999; revision received 27 February 2001; accepted for publication 1 March 2001.

*Assistant Professor, Dipartimento di Informatica e Sistemistica, Via Eudossiana 18; digiamberardino@dis.uniroma1.it.

†Professor, Dipartimento di Informatica e Sistemistica, Via Eudossiana 18; monaco@dis.uniroma1.it.

‡Ph.D. Student, Dipartimento di Informatica e Sistemistica, Via Eudossiana 18; ronchini@dis.uniroma1.it.

simplified structure was also assumed in Refs. 4, 6, and 7, where it is also shown that supercritical spinning velocity, that is, spin velocity greater than the natural frequency of the two-body system, guarantees self-centering of the cylinders but produces unstable whirling modes that could be stabilized by nonrotating damping.[7]

In this context a controller must ensure the fulfillment of the following requirements: stabilize the unstable whirling motion; ensure the centering of the cylinders, essential for the accuracy of the measures; and track the nominal orbit trajectory in the presence of atmospheric drag. In this paper, a control scheme is designed and proposed for the simultaneous stabilization of the cylinders, the orbit tracking,[8–10] and the drag effect rejection.[11–13] The methodological framework used here refers to the nonlinear regulation theory. The regulator proposed ensures asymptotic tracking of the desired output reference, from position measurements, in the presence of unknown parameter values.

The paper is structured as follows. First, the mathematical model is recalled, mainly referring to Ref. 7 for the cylinders dynamics and to Ref. 3 for the specific mission requirements. Then the model is modified into a standard form required by the nonlinear regulation theory, and the nonlinear controller is designed. Simulation results presented highlight the effectiveness of the proposed controller ensuring faster transient and higher tracking precision than traditional controllers; finally, a technique for EP violation detection is briefly discussed.

Mathematical Model

The system is composed of two corotating coaxial rigid cylinders, spinning at the same frequency around their symmetry axis and weakly coupled by means of two damped soft springs. The model is computed making reference to the following coordinate systems: 1) the main orthogonal inertial frame $Oxyz$, centered in O with the x and y axes in the equatorial plane and the z axis aligned with the planet polar axis, positive toward the north and 2) the two orthogonal rotating frames $\boldsymbol{\Gamma}_i\xi_i\eta_i\zeta_i$ and $\boldsymbol{\Gamma}_e\xi_e\eta_e\zeta_e$, centered in the centers of gravity of the cylinders, $\boldsymbol{\Gamma}_i$ and $\boldsymbol{\Gamma}_e$, respectively,

$$\boldsymbol{\Gamma}_i = \begin{pmatrix} x_i \\ y_i \\ z_i \end{pmatrix} \qquad \boldsymbol{\Gamma}_e = \begin{pmatrix} x_e \\ y_e \\ z_e \end{pmatrix} \tag{1}$$

and fixed with respect to the bodies. Once the Euler angles $\boldsymbol{\Phi}_i$ and $\boldsymbol{\Phi}_e$

$$\boldsymbol{\Phi}_i = \begin{pmatrix} \phi_i \\ \psi_i \\ \theta_i \end{pmatrix} \qquad \boldsymbol{\Phi}_e = \begin{pmatrix} \phi_e \\ \psi_e \\ \theta_e \end{pmatrix} \tag{2}$$

are introduced, $\boldsymbol{\Gamma}_i\xi_i\eta_i\zeta_i$ and $\boldsymbol{\Gamma}_e\xi_e\eta_e\zeta_e$ are related to the inertial frame by the rotation matrices $[\mathcal{R}_1(\phi_i), \mathcal{R}_2(\psi_i), \mathcal{R}_3(\theta_i)]$ and $[\mathcal{R}_1(\phi_e), \mathcal{R}_2(\psi_e), \mathcal{R}_3(\theta_e)]$, respectively. These matrices take the form

$$\mathcal{R}_1(\phi) = \begin{pmatrix} 1 & 0 & 0 \\ 0 & \cos\phi & \sin\phi \\ 0 & -\sin\phi & \cos\phi \end{pmatrix}$$

$$\mathcal{R}_2(\psi) = \begin{pmatrix} \cos\psi & 0 & -\sin\psi \\ 0 & 1 & 0 \\ \sin\psi & 0 & \cos\psi \end{pmatrix} \tag{3}$$

$$\mathcal{R}_3(\theta) = \begin{pmatrix} \cos\theta & \sin\theta & 0 \\ -\sin\theta & \cos\theta & 0 \\ 0 & 0 & 1 \end{pmatrix} \tag{4}$$

Because we assume that the axis of symmetry of each cylinder does not coincide with the rotation axis, we will denote by χ_i and χ_e (couple unbalances) the angles between them. Thus the frames $\boldsymbol{\Gamma}_i\xi_i\eta_i\zeta_i$ and $\boldsymbol{\Gamma}_e\xi_e\eta_e\zeta_e$ are not principals of inertia due to the angular errors χ_i and χ_e.

Each body has six degrees of freedom; therefore, six generalized coordinates per cylinder must be defined.

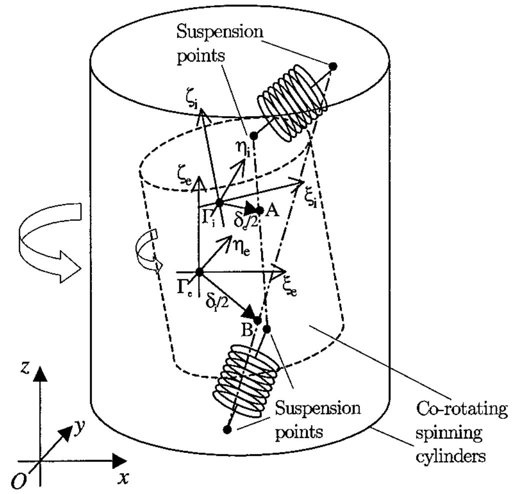

Fig. 1 Simplified mechanical structure of the satellite.

We assume that there is a misalignment of the suspension points of the springs and the gravity center of each body.

According to Fig. 1, we will denote by $\frac{1}{2}\boldsymbol{\delta}_i$ the distance between the center of mass and the middle point A of the suspension points for the inner body and by $\frac{1}{2}\boldsymbol{\delta}_e$ for the external body,

$$\boldsymbol{\delta}_i = \begin{pmatrix} \epsilon_{xi} \\ \epsilon_{yi} \\ \epsilon_{zi} \end{pmatrix} \qquad \boldsymbol{\delta}_e = \begin{pmatrix} \epsilon_{xe} \\ \epsilon_{ye} \\ \epsilon_{ze} \end{pmatrix} \tag{5}$$

The mathematical model is computed following the Lagrangian formulation

$$\frac{\mathrm{d}}{\mathrm{d}t}\left[\frac{\partial}{\partial\dot{\boldsymbol{q}}}(\mathcal{T}-\mathcal{U})\right] - \frac{\partial(\mathcal{T}-\mathcal{U})}{\partial\boldsymbol{q}} = \mathcal{Q} \tag{6}$$

where $\mathcal{Q}$ represent the nonconservative generalized forces (elastic and viscous damping forces, disturbances, and control inputs) and $\mathcal{T}$ and $\mathcal{U}$ represent the kinetic and potential energies.

Simulation Model

To compute the simulation model, we assume that $\mathcal{T}$ and $\mathcal{U}$ in Eq. (6) take the form

$$\mathcal{T} = \tfrac{1}{2}m_i|\dot{\boldsymbol{\Gamma}}_i|^2 + \tfrac{1}{2}m_e|\dot{\boldsymbol{\Gamma}}_e|^2 + \tfrac{1}{2}\Omega_i^T J_i\boldsymbol{\Omega}_i + \tfrac{1}{2}\Omega_e^T J_e\boldsymbol{\Omega}_e \tag{7}$$

$$\mathcal{U} = -G_u m_\oplus\left(\frac{m_i}{|\boldsymbol{\Gamma}_i|} + \frac{m_e}{|\boldsymbol{\Gamma}_e|}\right) \tag{8}$$

In the preceding expressions, m_i and m_e are the mass of the cylinders, and $J_i = \mathrm{diag}(J_{t_i}, J_{t_i}, J_{p_i})$ and $J_e = \mathrm{diag}(J_{t_e}, J_{t_e}, J_{p_e})$ are the inertial matrices in each body frame. The expressions for the components of $\boldsymbol{\Omega}_i$ and $\boldsymbol{\Omega}_e$, the angular velocity along the principal inertial axes, take the form

$$\boldsymbol{\Omega}_i = \mathcal{R}_2(\chi_i)\left[\mathcal{R}_3(\theta_i)\mathcal{R}_2(\psi_i)\begin{pmatrix} \dot{\phi}_i \\ 0 \\ 0 \end{pmatrix} + \mathcal{R}_3(\theta_i)\begin{pmatrix} 0 \\ \dot{\psi}_i \\ 0 \end{pmatrix} + \begin{pmatrix} 0 \\ 0 \\ \dot{\theta}_i \end{pmatrix}\right] \tag{9}$$

$$\boldsymbol{\Omega}_e = \mathcal{R}_2(\chi_e)\left[\mathcal{R}_3(\theta_e)\mathcal{R}_2(\psi_e)\begin{pmatrix} \dot{\phi}_e \\ 0 \\ 0 \end{pmatrix} + \mathcal{R}_3(\theta_e)\begin{pmatrix} 0 \\ \dot{\psi}_e \\ 0 \end{pmatrix} + \begin{pmatrix} 0 \\ 0 \\ \dot{\theta}_e \end{pmatrix}\right] \tag{10}$$

Performing the computations, we obtain

$$B_i(\boldsymbol{q}_i)\ddot{\boldsymbol{q}}_i + C_i(\boldsymbol{q}_i, \dot{\boldsymbol{q}}_i)\dot{\boldsymbol{q}}_i + g_i(\boldsymbol{q}_i) = \mathcal{Q}_i \tag{11}$$

$$B_e(\boldsymbol{q}_e)\ddot{\boldsymbol{q}}_e + C_e(\boldsymbol{q}_e, \dot{\boldsymbol{q}}_e)\dot{\boldsymbol{q}}_e + g_e(\boldsymbol{q}_e) = \mathcal{Q}_e \tag{12}$$

where

$$\boldsymbol{q}_i = \begin{pmatrix} \boldsymbol{\Gamma}_i \\ \boldsymbol{\Phi}_i \end{pmatrix} \qquad \boldsymbol{q}_e = \begin{pmatrix} \boldsymbol{\Gamma}_e \\ \boldsymbol{\Phi}_e \end{pmatrix} \qquad \boldsymbol{q} = \begin{pmatrix} \boldsymbol{q}_i \\ \boldsymbol{q}_e \end{pmatrix} \tag{13}$$

$B_i(\boldsymbol{q}_i)\ddot{\boldsymbol{q}}_i$ and $B_e(\boldsymbol{q}_e)\ddot{\boldsymbol{q}}_e$ are the inertial terms, $C_i(\boldsymbol{q}_i, \dot{\boldsymbol{q}}_i)\dot{\boldsymbol{q}}_i$ and $C_e(\boldsymbol{q}_e, \dot{\boldsymbol{q}}_e)\dot{\boldsymbol{q}}_e$ the Coriolis and centrifugal terms, and $g_i(\boldsymbol{q}_i)$ and $g_e(\boldsymbol{q}_e)$ the gravitational terms.

When Ref. 7 is followed for computing the expressions of $\mathcal{Q}_i$ and $\mathcal{Q}_e$, Eq. (11) and (12) take the form

$$\begin{aligned}
&\begin{bmatrix} B_{11}^i & 0 \\ 0 & B_{22}^i(\boldsymbol{\Phi}_i) \end{bmatrix} \begin{pmatrix} \ddot{\boldsymbol{\Gamma}}_i \\ \ddot{\boldsymbol{\Phi}}_i \end{pmatrix} + \begin{bmatrix} 0 & 0 \\ 0 & C_{22}^i(\boldsymbol{\Phi}_i) \end{bmatrix} \begin{pmatrix} \dot{\boldsymbol{\Gamma}}_i \\ \dot{\boldsymbol{\Phi}}_i \end{pmatrix} + \begin{bmatrix} G_{11}^i(\boldsymbol{\Gamma}_i) & 0 \\ 0 & 0 \end{bmatrix} \\
&\times \begin{pmatrix} \boldsymbol{\Gamma}_i \\ \boldsymbol{\Phi}_i \end{pmatrix} = -\begin{Bmatrix} K_\Gamma - H_i(\dot{\boldsymbol{\Phi}}_i) & 0 \\ \mathcal{M}_i(\boldsymbol{\Phi}_i)E_i[K_\Gamma - H_i(\dot{\boldsymbol{\Phi}}_i)] & 2\mathcal{N}_i(\boldsymbol{\Phi}_i)K_\Phi \end{Bmatrix} \\
&\times \begin{pmatrix} \Delta\boldsymbol{\Gamma} \\ \Delta\boldsymbol{\Phi} \end{pmatrix} - \begin{bmatrix} C_\Gamma & 0 \\ \mathcal{M}_i(\boldsymbol{\Phi}_i)E_iC_\Gamma & 2\mathcal{N}_i(\boldsymbol{\Phi}_i)C_\Phi \end{bmatrix} \\
&\times \begin{pmatrix} \Delta\dot{\boldsymbol{\Gamma}} \\ \Delta\dot{\boldsymbol{\Phi}} \end{pmatrix} + \begin{bmatrix} I & 0 \\ \mathcal{M}_i(\boldsymbol{\Phi}_i)U_i' & I \end{bmatrix} \begin{pmatrix} \boldsymbol{u}_{\Gamma_i} \\ \boldsymbol{u}_{\Phi_i} \end{pmatrix}
\end{aligned} \tag{14}$$

and

$$\begin{aligned}
&\begin{bmatrix} B_{11}^e & 0 \\ 0 & B_{22}^e(\boldsymbol{\Phi}_e) \end{bmatrix} \begin{pmatrix} \ddot{\boldsymbol{\Gamma}}_e \\ \ddot{\boldsymbol{\Phi}}_e \end{pmatrix} + \begin{bmatrix} 0 & 0 \\ 0 & C_{22}^e(\boldsymbol{\Phi}_e) \end{bmatrix} \begin{pmatrix} \dot{\boldsymbol{\Gamma}}_e \\ \dot{\boldsymbol{\Phi}}_e \end{pmatrix} + \begin{bmatrix} G_{11}^e(\boldsymbol{\Gamma}_e) & 0 \\ 0 & 0 \end{bmatrix} \\
&\times \begin{pmatrix} \boldsymbol{\Gamma}_e \\ \boldsymbol{\Phi}_e \end{pmatrix} = \begin{Bmatrix} K_\Gamma - H_e(\dot{\boldsymbol{\Phi}}_e) & 0 \\ \mathcal{M}_e(\boldsymbol{\Phi}_e)E_e[K_\Gamma - H_e(\dot{\boldsymbol{\Phi}}_e)] & 2\mathcal{N}_e(\boldsymbol{\Phi}_e)K_\Phi \end{Bmatrix} \\
&\times \begin{pmatrix} \Delta\boldsymbol{\Gamma} \\ \Delta\boldsymbol{\Phi} \end{pmatrix} + \begin{bmatrix} C_\Gamma & 0 \\ \mathcal{M}_e(\boldsymbol{\Phi}_e)E_eC_\Gamma & 2\mathcal{N}_e(\boldsymbol{\Phi}_e)C_\Phi \end{bmatrix} \begin{pmatrix} \Delta\dot{\boldsymbol{\Gamma}} \\ \Delta\dot{\boldsymbol{\Phi}} \end{pmatrix} \\
&- \begin{bmatrix} I & 0 \\ \mathcal{M}_e(\boldsymbol{\Phi}_e)U_i'' & I \end{bmatrix} \begin{pmatrix} \boldsymbol{u}_{\Gamma_i} \\ \boldsymbol{u}_{\Phi_i} \end{pmatrix} + \begin{bmatrix} I \\ \mathcal{M}_e(\boldsymbol{\Phi}_e)U_d \end{bmatrix} d \\
&+ \begin{bmatrix} I & 0 \\ \mathcal{M}_e(\boldsymbol{\Phi}_e)U_e & I \end{bmatrix} \begin{pmatrix} \boldsymbol{u}_{\Gamma_e} \\ \boldsymbol{u}_{\Phi_e} \end{pmatrix} + \begin{pmatrix} \boldsymbol{w}_{\Gamma_e} \\ \boldsymbol{w}_{\Phi_e} \end{pmatrix}
\end{aligned} \tag{15}$$

where $H_i(\dot{\boldsymbol{\Phi}}_i)$ and $H_e(\dot{\boldsymbol{\Phi}}_e)$ are the gyroscopic matrices computed from

$$c_t\boldsymbol{\omega}_i \times \Delta\boldsymbol{\Gamma} = c_t\tilde{\omega}_i\Delta\Gamma = H_i(\dot{\boldsymbol{\Phi}}_i)\Delta\boldsymbol{\Gamma} \tag{16}$$

$$c_t\boldsymbol{\omega}_e \times \Delta\boldsymbol{\Gamma} = c_t\tilde{\omega}_e\Delta\Gamma = H_e(\dot{\boldsymbol{\Phi}}_e)\Delta\boldsymbol{\Gamma} \tag{17}$$

where $\boldsymbol{\omega}_i$ and $\boldsymbol{\omega}_e$ are the angular velocities in the inertial frame, given by

$$\boldsymbol{\omega}_i = \mathcal{R}_1^T(\phi_i)\mathcal{R}_2^T(\psi_i)\mathcal{R}_3^T(\theta_i)\boldsymbol{\Omega}_i \tag{18}$$

$$\boldsymbol{\omega}_e = \mathcal{R}_1^T(\phi_e)\mathcal{R}_2^T(\psi_e)\mathcal{R}_3^T(\theta_e)\boldsymbol{\omega}_e \tag{19}$$

and $\tilde{\omega}_i$ and $\tilde{\omega}_e$ are the dyadic matrices related to $\boldsymbol{\omega}_i$ and $\boldsymbol{\omega}_e$. K_Γ and K_Φ are the translational and rotational diagonal stiffness matrices; C_Γ and C_Φ are the translational and rotational diagonal damping matrices; E_i and E_e are the dyadic matrices related to $\boldsymbol{\gamma}_i$ and $\boldsymbol{\gamma}_e$, respectively; U_i', U_i'', U_e, and U_d are the dyadic matrices, which take into account not centering the forces with respect the gravity centers; and $\mathcal{M}_i(\boldsymbol{\Phi}_i)$ $\mathcal{M}_e(\boldsymbol{\Phi}_e)$, $\mathcal{N}_i(\boldsymbol{\Phi}_i)$, and $\mathcal{N}_e(\boldsymbol{\Phi}_e)$ are particular rotation matrices, which relate the reference frames $\boldsymbol{\Gamma}_i\xi_i\eta_i\zeta_i$ and $\boldsymbol{\Gamma}_e\xi_e\eta_e\zeta_e$ to nonorthogonal frames in which some of the generalized forces act.[7] $\Delta\boldsymbol{\Gamma}$ is given by

$$\begin{aligned}
\Delta\boldsymbol{\Gamma} &= \Delta\Gamma_l + \Delta\Gamma_u = 2(\boldsymbol{\Gamma}_i - \boldsymbol{\Gamma}_e) - \gamma_i^l - \gamma_i^u + \gamma_e^l + \gamma_e^u \\
&= 2(\boldsymbol{\Gamma}_i - \boldsymbol{\Gamma}_e) - \boldsymbol{\gamma}_i + \boldsymbol{\gamma}_e
\end{aligned}$$

where $\Delta\Gamma_l$ and $\Delta\Gamma_u$ are the displacements of the lower and upper springs, respectively, and $\boldsymbol{\gamma}_i = \gamma_i^l + \gamma_i^u$ and $\boldsymbol{\gamma}_e = \gamma_e^l + \gamma_e^u$ denote $\boldsymbol{\delta}_i$ and $\boldsymbol{\delta}_e$ in the inertial frame. Their detailed expression can be computed from

$$\boldsymbol{\gamma}_i = \begin{pmatrix} \gamma_{x_i} \\ \gamma_{y_i} \\ \gamma_{z_i} \end{pmatrix} = \mathcal{R}_1^T(\phi_i)\mathcal{R}_2^T(\psi_i)\mathcal{R}_3^T(\theta_i)\boldsymbol{\delta}_i \tag{20}$$

$$\boldsymbol{\gamma}_e = \begin{pmatrix} \gamma_{x_e} \\ \gamma_{y_e} \\ \gamma_{z_e} \end{pmatrix} = \mathcal{R}_1^T(\phi_e)\mathcal{R}_2^T(\psi_e)\mathcal{R}_3^T(\theta_e)\boldsymbol{\delta}_e \tag{21}$$

$\Delta\boldsymbol{\Phi}$ is $\boldsymbol{\Phi}_i - \boldsymbol{\Phi}_e$. Here d is the drag force acting on the external cylinder; it is a periodic disturbance, which in our study takes the form

$$d = \begin{pmatrix} d_1 \sin\omega_o t + d_2 \sin 2\omega_o t \\ -d_1 \cos\omega_o t - d_2 \cos 2\omega_o t \\ 0 \end{pmatrix} \tag{22}$$

that is, it is composed by the first two terms of the Fourier series expansion, with $\omega_o/2\pi$ the orbital frequency. Note that $\boldsymbol{w}_{\Gamma_e}$ and $\boldsymbol{w}_{\Phi_e}$ could contain all of the other external undesired perturbation effects, such as nonuniform thermal expansion, thermal change of spring's stiffness, thermal noise, magnetic interactions, electrostatic effects and so on and that $\boldsymbol{u}_{\Gamma_e}$, $\boldsymbol{u}_{\Phi_e}$, $\boldsymbol{u}_{\Gamma_i}$, and $\boldsymbol{u}_{\Phi_i}$ are the control inputs.

The detailed expressions of the terms in Eq. (14) and (15) are reported in Appendix A.

Control Model

To achieve the controller's Synthesis, a simpler model is computed by using simplified expressions for $\mathcal{T}$ and $\mathcal{Q}$ in Eq. (6).

Assumption 1, small angles: Very small angles χ_i, χ_e, ϕ_i, ϕ_e, ψ_i, and ψ_e (within about $\frac{1}{10}$ deg) are assumed; this yields the following simplifications:

1) The kinetic energy $\mathcal{T}$ reduces to the simplified expression $\mathcal{T}'$

$$\begin{aligned}
\mathcal{T}' &= \tfrac{1}{2}\Omega_i^T J_i\boldsymbol{\Omega}_i + \tfrac{1}{2}\Omega_e^T J_e\boldsymbol{\Omega}_e = \tfrac{1}{2}m_i\left(\dot{x}_i^2 + \dot{y}_i^2 + \dot{z}_i^2\right) \\
&\quad + \tfrac{1}{2}m_e\left(\dot{x}_e^2 + \dot{y}_e^2 + \dot{z}_e^2\right) + \tfrac{1}{2}\Big[J_{t_i}\dot{\phi}_i^2 + J_{t_i}\dot{\psi}_i^2 + J_{t_e}\dot{\phi}_e^2 + J_{t_e}\dot{\psi}_e^2 \\
&\quad + \left(J_{p_i} + J_{t_i}\chi_i^2\right)\dot{\theta}_i^2 + \left(J_{p_e} + J_{t_e}\chi_e^2\right)\dot{\theta}_e^2\Big] + J_{p_i}\dot{\phi}_i\psi_i\dot{\theta}_i \\
&\quad + J_{p_e}\dot{\phi}_e\psi_e\dot{\theta}_e + \left(J_{p_i} - J_{t_i}\right)\left(\dot{\phi}_i\cos\theta_i + \dot{\psi}_i\sin\theta_i\right)\dot{\theta}_i\chi_i \\
&\quad + \left(J_{p_e} - J_{t_e}\right)\left(\dot{\phi}_e\cos\theta_e + \dot{\psi}_e\sin\theta_e\right)\dot{\theta}_e\chi_e
\end{aligned} \tag{23}$$

2) $H_i(\dot{\boldsymbol{\Phi}}_i)$ and $H_e(\dot{\boldsymbol{\Phi}}_e)$ take the form

$$H_i(\dot{\boldsymbol{\Phi}}_i) = c_t\dot{\theta}_i \begin{pmatrix} 0 & -1 & 0 \\ 1 & 0 & 0 \\ 0 & 0 & 0 \end{pmatrix} \tag{24}$$

$$H_e(\dot{\boldsymbol{\Phi}}_e) = c_t\dot{\theta}_e \begin{pmatrix} 0 & -1 & 0 \\ 1 & 0 & 0 \\ 0 & 0 & 0 \end{pmatrix} \tag{25}$$

where c_t denotes the spring's translational damping coefficient.

3) Also $\boldsymbol{\gamma}_i$ and $\boldsymbol{\gamma}_e$ reduce to

$$\boldsymbol{\gamma}_i = \begin{pmatrix} \epsilon_{x_i}\cos\theta_i - \epsilon_{y_i}\sin\theta_i \\ \epsilon_{x_i}\sin\theta_i + \epsilon_{y_i}\cos\theta_i \\ \epsilon_{z_i} \end{pmatrix} \qquad \boldsymbol{\gamma}_e = \begin{pmatrix} \epsilon_{x_e}\cos\theta_e - \epsilon_{y_e}\sin\theta_e \\ \epsilon_{x_e}\sin\theta_e + \epsilon_{y_e}\cos\theta_e \\ \epsilon_{z_e} \end{pmatrix} \tag{26}$$

4) $\mathcal{M}_i(\boldsymbol{\Phi}_i)$, $\mathcal{M}_e(\boldsymbol{\Phi}_e)$, $\mathcal{N}_i(\boldsymbol{\Phi}_i)$, and $\mathcal{N}_e(\boldsymbol{\Phi}_e)$ reduce to

$$\mathcal{M}_i(\boldsymbol{\Phi}_i) = \mathcal{M}_e(\boldsymbol{\Phi}_e) = \mathcal{N}_i(\boldsymbol{\Phi}_i) = \mathcal{N}_e(\boldsymbol{\Phi}_e) = \begin{pmatrix} 1 & 0 & 0 \\ 0 & 1 & 0 \\ 0 & 0 & 1 \end{pmatrix} \tag{27}$$

Assumption 2, small coupling torques: The torques due to the eccentricities are assumed to be negligible; it follows that

$$U_i' = 0 \qquad U_i'' = 0 \qquad U_e = 0$$
$$U_d = 0 \qquad E_i = 0 \qquad E_e = 0 \tag{28}$$

Assumption 3, small torque disturbances: We neglect the disturbances $\boldsymbol{w}_{\Gamma_e}$ and $\boldsymbol{w}_{\Phi_e}$

$$\boldsymbol{w}_{\Gamma_e} = 0 \qquad \boldsymbol{w}_{\Phi_e} = 0 \tag{29}$$

Moreover, the inputs to the control model are $\boldsymbol{u}_{\Gamma_i}$ and $\boldsymbol{u}_{\Gamma_e}$ ($\boldsymbol{u}_{\Phi_i} = 0$ and $\boldsymbol{u}_{\Phi_e} = 0$) in consequence of the design constraints (no active attitude control).

Rewriting the drag force Eq. (22) as

$$d = \mathcal{D}\boldsymbol{w}_d = \begin{pmatrix} 0 & 1 & 0 & 1 \\ -1 & 0 & -1 & 0 \\ 0 & 0 & 0 & 0 \end{pmatrix} \begin{pmatrix} w_{d_x^1} \\ w_{d_y^1} \\ w_{d_x^2} \\ w_{d_y^2} \end{pmatrix}$$
$$= \begin{pmatrix} 0 & 1 & 0 & 1 \\ -1 & 0 & -1 & 0 \\ 0 & 0 & 0 & 0 \end{pmatrix} \begin{pmatrix} d_1 \cos\omega_o t \\ d_1 \sin\omega_o t \\ d_2 \cos 2\omega_o t \\ d_2 \sin 2\omega_o t \end{pmatrix} \tag{30}$$

the control model can be computed from Eqs. (14) and (15), under Assumptions 1–3, yielding

$$m_i \ddot{\boldsymbol{\Gamma}}_i = -G_{11}^i(\boldsymbol{\Gamma}_i)\boldsymbol{\Gamma}_i - [K_\Gamma - H_i(\dot{\boldsymbol{\Phi}}_i)]\Delta\boldsymbol{\Gamma} - C_\Gamma \Delta\dot{\boldsymbol{\Gamma}} + \boldsymbol{u}_{\Gamma_i}$$
$$\ddot{\boldsymbol{\Phi}}_i = -\Lambda_i(\dot{\boldsymbol{\Phi}}_i)\dot{\boldsymbol{\Phi}}_i + 2\Sigma_i(-K_\Phi \Delta\boldsymbol{\Phi} - C_\Phi \Delta\dot{\boldsymbol{\Phi}}) \tag{31}$$
$$m_e \ddot{\boldsymbol{\Gamma}}_e = -G_{11}^e(\boldsymbol{\Gamma}_e)\boldsymbol{\Gamma}_e + [K_\Gamma - H_e(\dot{\boldsymbol{\Phi}}_e)]\Delta\boldsymbol{\Gamma} + C_\Gamma \Delta\dot{\boldsymbol{\Gamma}} - \boldsymbol{u}_{\Gamma_i} + \boldsymbol{u}_{\Gamma_e} + \mathcal{D}\boldsymbol{w}_d$$
$$\ddot{\boldsymbol{\Phi}}_e = -\Lambda_e(\dot{\boldsymbol{\Phi}}_e)\dot{\boldsymbol{\Phi}}_e + 2\Sigma_e(K_\Phi \Delta\boldsymbol{\Phi} + C_\Phi \Delta\dot{\boldsymbol{\Phi}}) \tag{32}$$
$$\boldsymbol{y} = \begin{pmatrix} \boldsymbol{\Gamma}_i - \boldsymbol{\Gamma}_e \\ \boldsymbol{\Gamma}_e \end{pmatrix} \tag{33}$$

In conclusion, the dynamics of the system takes the form

$$\dot{\boldsymbol{x}} = f(\boldsymbol{x}) + g(\boldsymbol{x})\boldsymbol{u} + p(\boldsymbol{x})\boldsymbol{w} \tag{34}$$
$$\boldsymbol{y} = h(\boldsymbol{x}) \tag{35}$$

with respect to the state and input vectors

$$\boldsymbol{x} = \begin{pmatrix} \boldsymbol{\Gamma}_i \\ \boldsymbol{\Phi}_i \\ \boldsymbol{\Gamma}_e \\ \boldsymbol{\Phi}_e \\ \dot{\boldsymbol{\Gamma}}_i \\ \dot{\boldsymbol{\Phi}}_i \\ \dot{\boldsymbol{\Gamma}}_e \\ \dot{\boldsymbol{\Phi}}_e \end{pmatrix} \qquad \boldsymbol{u} = \begin{pmatrix} \boldsymbol{u}_{\Gamma_i} \\ \boldsymbol{u}_{\Gamma_e} \end{pmatrix} \qquad \boldsymbol{w} = \boldsymbol{w}_d \tag{36}$$

where the expression of the matrices in Eqs. (31–33) are given in Appendix B. The whole dynamics is nonlinear due to depending on the state by the matrices $G_{11}^i(\boldsymbol{\Gamma}_i)$, $G_{11}^e(\boldsymbol{\Gamma}_e)$, $H_i(\dot{\boldsymbol{\Phi}}_i)$, $H_e(\dot{\boldsymbol{\Phi}}_e)$, $\Lambda_i(\boldsymbol{\Phi}_i)$, and $\Lambda_e(\boldsymbol{\Phi}_e)$.

Design of the Controller

In this section the error feedback regulator will be computed on the basis of the approximated control model developed in the preceding section. First a review of nonlinear regulation is in order.

Nonlinear Regulation

Following the approach developed in Ref. 1, let us consider the system

$$\dot{\boldsymbol{x}} = f(\boldsymbol{x}) + g(\boldsymbol{x})\boldsymbol{u} + \tilde{p}(\boldsymbol{x})\boldsymbol{d} \tag{37}$$
$$\boldsymbol{y} = h(\boldsymbol{x}) \tag{38}$$

with $\boldsymbol{y}_r$ the output reference to be tracked and $\boldsymbol{d}$ the vector of disturbances. Let us introduce a nonlinear autonomous dynamic system, called the exosystem, described by the differential equation

$$\dot{\boldsymbol{w}} = s(\boldsymbol{w}) \tag{39}$$

which can generate both the reference $\boldsymbol{y}_r$ and the disturbances $\boldsymbol{d}$. Then we can write

$$\boldsymbol{y}_r = -\boldsymbol{q}(\boldsymbol{w}) \tag{40}$$

and, incorporating into a single set of equations the exosystem and the plant model, we obtain

$$\dot{\boldsymbol{x}} = f(\boldsymbol{x}) + g(\boldsymbol{x})\boldsymbol{u} + p(\boldsymbol{x})\boldsymbol{w} \tag{41}$$
$$\dot{\boldsymbol{w}} = s(\boldsymbol{w}) \tag{42}$$
$$e = h(\boldsymbol{x}) + \boldsymbol{q}(\boldsymbol{w}) \tag{43}$$

where e is the output tracking error. Such a model will be referred to as the standard form. As usual in control theory, it is assumed that the plant (37–38), with m inputs and m outputs, has a state $\boldsymbol{x}$ defined in a neighborhood of the origin $\mathbb{R}^n$, as well as the state $\boldsymbol{w}$ of the exosystem being defined in a neighborhood of the origin of $\mathbb{R}^s$. Moreover, the natural hypotheses of the problem are the smoothness of $f(\boldsymbol{x})$, $g(\boldsymbol{x})$, $h(\boldsymbol{x})$, $s(\boldsymbol{w})$ and $\boldsymbol{q}(\boldsymbol{w})$, with $f(0) = 0$, $h(0) = 0$, and $\boldsymbol{q}(0) = 0$, so that system (41–43) has an equilibrium state $(\boldsymbol{x}, \boldsymbol{w}) = (0, 0)$, for $\boldsymbol{u} = 0$, corresponding to zero error $e(t)$.

The control action can be provided either by state feedback or by output feedback. A fundamental role is played by the linear approximation of Eqs. (41–43) at $(\boldsymbol{x}, \boldsymbol{w}) = (0, 0)$,

$$A = \left.\frac{\partial f}{\partial \boldsymbol{x}}\right|_{x=0} \qquad B = g(0) \qquad P = p(0) \qquad S = \left.\frac{\partial s}{\partial \boldsymbol{w}}\right|_{w=0}$$
$$C = \left.\frac{\partial h}{\partial \boldsymbol{x}}\right|_{x=0} \qquad Q = \left.\frac{\partial \boldsymbol{q}}{\partial \boldsymbol{w}}\right|_{w=0} \tag{44}$$

State Feedback Regulator

The problem consists of finding a control $\boldsymbol{u}$, function of $\boldsymbol{x}$ and $\boldsymbol{w}$

$$\boldsymbol{u} = \alpha(\boldsymbol{x}, \boldsymbol{w}), \qquad \text{with} \qquad \alpha(0, 0) = 0 \tag{45}$$

such that the closed-loop system

$$\dot{\boldsymbol{x}} = f(\boldsymbol{x}) + g(\boldsymbol{x})\alpha(\boldsymbol{x}, 0) \tag{46}$$

has the equilibrium $\boldsymbol{x} = 0$ locally asymptotically stable and for any initial condition $[\boldsymbol{x}(0), \boldsymbol{w}(0)]$ in a neighborhood of (0, 0) the system (41–43) satisfies

$$\lim_{t\to\infty} e(t) = 0 \tag{47}$$

For the solution of the state feedback regulator problem we can use the following result (Ref. 1, Theorem 2.5).

Hypothesis 1: The state $w = 0$ is a stable equilibrium of the exosystem, and there is an open neighborhood where every point is Poisson stable.

Hypothesis 2: The pair (A, B) is stabilizable, that is, the eigenvalues belonging to the uncontrollable subsystem have a negative real part. Then the state feedback regulator problem is solvable if and only if there exist C^k $(k \geq 2)$ mappings $\boldsymbol{x} = \pi(w)$ with $\pi(0) = 0$, and $\boldsymbol{u} = c(\boldsymbol{w})$, with $c(0) = 0$, both defined in a neighborhood of the origin, satisfying the conditions

$$\frac{\partial \pi}{\partial \boldsymbol{w}} s(\boldsymbol{w}) = f[\pi(\boldsymbol{w})] + g[\pi(\boldsymbol{w})]c(\boldsymbol{w}) + p[\pi(\boldsymbol{w})]\boldsymbol{w} \tag{48}$$
$$0 = h[\pi(\boldsymbol{w})] + \boldsymbol{q}(\boldsymbol{w}) \tag{49}$$

The solution takes the form

$$\alpha(\boldsymbol{x}, \boldsymbol{w}) = c(\boldsymbol{w}) + K[\boldsymbol{x} - \pi(\boldsymbol{w})] \tag{50}$$

where K is to be designed to ensure that $A + BK$ has all eigenvalues with negative real parts.

Output Feedback Regulator

The case that only the output measures are available the feedback control takes the form

$$\dot{\xi} = \eta(\boldsymbol{\xi}, e) \tag{51}$$

$$u = \theta(\boldsymbol{\xi}) \tag{52}$$

with $\eta(0, 0) = 0$ and $\theta(0) = 0$. The functions $\eta(\boldsymbol{\xi}, e)$ and $\theta(\boldsymbol{\xi})$ must be computed to ensure that the closed-loop system

$$\dot{\boldsymbol{x}} = f(\boldsymbol{x}) + g(\boldsymbol{x})\theta(\boldsymbol{\xi}) \tag{53}$$

$$\dot{\xi} = \eta[\boldsymbol{\xi}, h(\boldsymbol{x})] \tag{54}$$

has a locally asymptotically stable equilibrium at the origin, and for any initial condition in a neighborhood of $(\boldsymbol{x}, \boldsymbol{\xi}, \boldsymbol{w}) = (0, 0, 0)$, the solution of Eqs. (41–43) satisfies

$$\lim_{t\to\infty} e(t) = 0 \tag{55}$$

For the solution of the problem, we can use the following result (Ref. 1, Theorem 2.10). We use Hypotheses 1 and 2 and the following hypothesis for the result.

Hypothesis 3: The pair (A_e, C_e) is detectable, where

$$A_e = \begin{pmatrix} A & P \\ 0 & S \end{pmatrix} \qquad C_e = (C \quad Q) \tag{56}$$

that is, the eigenvalues belonging to the unobservable subsystem have a negative real part. Then the output feedback regulation problem is solvable if and only if there exist C^k $(k \geq 2)$ mappings $\boldsymbol{x} = \pi(\boldsymbol{w})$ with $\pi(0) = 0$, and $\boldsymbol{u} = c(\boldsymbol{w})$, with $c(0) = 0$, both defined in a neighborhood of the origin, satisfying the conditions

$$\frac{\partial \pi}{\partial \boldsymbol{w}} s(\boldsymbol{w}) = f[\pi(\boldsymbol{w})] + g[\pi(\boldsymbol{w})]c(\boldsymbol{w}) + p[\pi(\boldsymbol{w})]\boldsymbol{w} \tag{57}$$

$$0 = h[\pi(\boldsymbol{w})] + \boldsymbol{q}(\boldsymbol{w}) \tag{58}$$

In this case, it is possible to show that solution (51) and (52) takes the form

$$\dot{\xi}_1 = f(\xi_1) + p(\xi_1)\xi_2 + g(\xi_1)[c(\xi_2) + K\xi_1 - K\pi(\xi_2)] - G_1[h(\xi_1) + \boldsymbol{q}(\xi_2) - e] \tag{59}$$

$$\dot{\xi}_2 = s(\xi_2) - G_2[h(\xi_1) + \boldsymbol{q}(\xi_2) - e] \tag{60}$$

$$\theta(\xi_1, \xi_2) = c(\xi_2) + K[\xi_1 - \pi(\xi_2)] \tag{61}$$

where K and $G = (G_1^T \;\; G_2^T)^T$ are designed to ensure that $A + BK$ and $A_e - GC_e$ have all eigenvalues with a negative real part.

Reduction to Standard Form

The model described by Eqs. (31–33) has no equilibrium points at the origin, due to the presence of gravitational terms; then, two appropriate changes of variable must be considered. A first one is needed to translate the origin of the reference frame on the equilibrium nominal orbital trajectory,

$$\boldsymbol{x}_i = \tilde{\boldsymbol{x}}_i + \boldsymbol{w}_x^0 \qquad \boldsymbol{y}_i = \tilde{\boldsymbol{y}}_i + \boldsymbol{w}_y^0$$

$$\boldsymbol{x}_e = \tilde{\boldsymbol{x}}_e + \boldsymbol{w}_x^0 \qquad \boldsymbol{y}_e = \tilde{\boldsymbol{y}}_e + \boldsymbol{w}_y^0 \tag{62}$$

where $\boldsymbol{w}_x^0 = R\cos\omega_o t$ and $w_y^0 = R\sin\omega_o t$; then, we set

$$\theta_i = \tilde{\theta}_i + \omega_s t \tag{63}$$

$$\theta_e = \tilde{\theta}_e + \omega_s t \tag{64}$$

to place the spin equilibrium to zero. This allows us to introduce the variables $\boldsymbol{w}_x^s = \cos\omega_s t$ and $\boldsymbol{w}_y^s = \sin\omega_s t$, where $\omega_s = 2$ Hz, thus defining

$$\boldsymbol{w}_s = \begin{pmatrix} w_x^s \\ w_y^s \end{pmatrix} \tag{65}$$

Setting

$$\tilde{\Gamma}_i = \begin{pmatrix} \tilde{x}_i \\ \tilde{y}_i \\ z_i \end{pmatrix} = \boldsymbol{\Gamma}_i - \begin{pmatrix} w_x^0 \\ w_y^0 \\ 0 \end{pmatrix} \tag{66}$$

$$\tilde{\Gamma}_e = \begin{pmatrix} \tilde{x}_e \\ \tilde{y}_e \\ z_e \end{pmatrix} = \boldsymbol{\Gamma}_e - \begin{pmatrix} w_x^0 \\ w_y^0 \\ 0 \end{pmatrix} \tag{67}$$

$$\tilde{\Phi}_i = \begin{pmatrix} \phi_i \\ \psi_i \\ \tilde{\theta}_i \end{pmatrix} = \begin{pmatrix} \phi_i \\ \psi_i \\ \theta_i \end{pmatrix} - \begin{pmatrix} 0 \\ 0 \\ \omega_s t \end{pmatrix} \tag{68}$$

$$\tilde{\Phi}_e = \begin{pmatrix} \phi_e \\ \psi_e \\ \tilde{\theta}_e \end{pmatrix} = \begin{pmatrix} \phi_e \\ \psi_e \\ \theta_e \end{pmatrix} - \begin{pmatrix} 0 \\ 0 \\ \omega_s t \end{pmatrix} \tag{69}$$

we define the matrix $\mathcal{H}$ and the vectors $\mathbf{Y}$ and $\boldsymbol{w}_o$ as follows:

$$\ddot{\tilde{\Gamma}}_i - \ddot{\boldsymbol{\Gamma}}_i = \ddot{\tilde{\Gamma}}_e - \ddot{\boldsymbol{\Gamma}}_e = \begin{pmatrix} \omega_o^2 & 0 & 0 & 0 & 0 \\ 0 & \omega_o^2 & 0 & 0 & 0 \\ 0 & 0 & 0 & 0 & 0 \end{pmatrix} \times \begin{pmatrix} R\cos\omega_o t \\ R\sin\omega_o t \\ R^2\cos^2\omega_o t \\ R^2\sin^2\omega_o t \\ R^2\cos\omega_o t\sin\omega_o t \end{pmatrix} = \mathcal{H}\begin{pmatrix} w_x^0 \\ w_y^0 \\ w_{x2}^0 \\ w_{y2}^0 \\ w_{xy}^0 \end{pmatrix} = \mathcal{H}\boldsymbol{w}_o \tag{70}$$

$$\dot{\tilde{\Phi}}_i - \dot{\boldsymbol{\Phi}}_i = \dot{\tilde{\Phi}}_e - \dot{\boldsymbol{\Phi}}_e = \begin{pmatrix} 0 \\ 0 \\ \omega_s \end{pmatrix} = \mathbf{Y} \tag{71}$$

Now, we make the following further assumptions.

Assumption 4, gravitational forces: In place of the exact expression of the gravitational forces $G_{11}^i(\boldsymbol{\Gamma}_i)\boldsymbol{\Gamma}_i$ and $G_{11}^e(\boldsymbol{\Gamma}_e)\boldsymbol{\Gamma}_e$, let us assume the following development:

$$G_{11}^i(\boldsymbol{\Gamma}_i)\boldsymbol{\Gamma}_i \cong \mathcal{G}_i(\tilde{\Gamma}_i)\tilde{\Gamma}_i + \mathcal{F}_i(\tilde{\Gamma}_i)\boldsymbol{w}_o \tag{72}$$

$$G_{11}^e(\boldsymbol{\Gamma}_e)\boldsymbol{\Gamma}_e \cong \mathcal{G}_e(\tilde{\Gamma}_e)\tilde{\Gamma}_e + \mathcal{F}_e(\tilde{\Gamma}_e)\boldsymbol{w}_o \tag{73}$$

obtained by a second-order multivariate Taylor series expansion, where

$$\mathcal{G}_i(\tilde{\Gamma}_i) = \frac{G_u m_\oplus m_i}{\left(\sqrt{\tilde{x}_i^2 + \tilde{y}_i^2 + z_i^2 + R^2}\right)^3}$$

$$\mathcal{G}_e(\tilde{\Gamma}_e) = \frac{G_u m_\oplus m_e}{\left(\sqrt{\tilde{x}_e^2 + \tilde{y}_e^2 + z_e^2 + R^2}\right)^3} \tag{74}$$

The expression of $\mathcal{F}_i(\tilde{\Gamma}_i)$ and $\mathcal{F}_e(\tilde{\Gamma}_e)$ is detailed in Appendix C.

Assumption 5, small spin displacement: We assume $\tilde{\theta}_e \cong \tilde{\theta}_i$ in the simplified expression of $\boldsymbol{\gamma}_e$ and $\boldsymbol{\gamma}_i$, thus obtaining

$$\gamma_e - \gamma_i = \begin{pmatrix} \cos\tilde{\theta}_e & -\sin\tilde{\theta}_e & 0 \\ \sin\tilde{\theta}_e & \cos\tilde{\theta}_e & 0 \\ 0 & 0 & 1 \end{pmatrix} \boldsymbol{w}_p \tag{75}$$

$$\dot{\gamma}_e - \dot{\gamma}_i = \left(\dot{\tilde{\theta}}_e + \omega_s\right) \begin{pmatrix} -\sin\tilde{\theta}_e & -\cos\tilde{\theta}_e & 0 \\ \cos\tilde{\theta}_e & -\sin\tilde{\theta}_e & 0 \\ 0 & 0 & 0 \end{pmatrix} \boldsymbol{w}_p \tag{76}$$

where

$$\boldsymbol{w}_p = \begin{pmatrix} w_\alpha \\ w_\beta \\ w_\gamma \end{pmatrix} = \begin{bmatrix} \left(\epsilon_{x_e} - \epsilon_{x_i}\right)\cos\omega_s t - \left(\epsilon_{y_e} - \epsilon_{y_i}\right)\sin\omega_s t \\ \left(\epsilon_{x_e} - \epsilon_{x_i}\right)\sin\omega_s t + \left(\epsilon_{y_e} - \epsilon_{y_i}\right)\cos\omega_s t \\ \epsilon_{z_e} - \epsilon_{z_i} \end{bmatrix} \tag{77}$$

In conclusion, we obtain

$$\begin{aligned} &2[K_\Gamma - H_i(\dot{\tilde{\Phi}}_i)]\left(\tilde{\Gamma}_i - \tilde{\Gamma}_e + \tfrac{1}{2}\gamma_e - \tfrac{1}{2}\gamma_i\right) \\ &\quad + 2C_\Gamma\left(\dot{\tilde{\Gamma}}_i - \dot{\tilde{\Gamma}}_e + \tfrac{1}{2}\dot{\gamma}_e - \tfrac{1}{2}\dot{\gamma}_i\right) - 2[K_\Gamma - H_i(\dot{\tilde{\Phi}}_i)](\tilde{\Gamma}_i - \tilde{\Gamma}_e) \\ &\quad \cong [K_\Gamma - H_i(\dot{\tilde{\Phi}}_e)](\gamma_e - \gamma_i) + 2C_\Gamma(\dot{\tilde{\Gamma}}_i - \dot{\tilde{\Gamma}}_e) + C_\Gamma(\dot{\gamma}_e - \dot{\gamma}_i) \\ &\quad \cong \mathcal{P}(\tilde{\Phi}_e)\boldsymbol{w}_p + 2C_\Gamma(\dot{\tilde{\Gamma}}_i - \dot{\tilde{\Gamma}}_e) \end{aligned} \tag{78}$$

and

$$\begin{aligned} &2[K_\Gamma - H_e(\dot{\tilde{\Phi}}_e)]\left(\tilde{\Gamma}_i - \tilde{\Gamma}_e + \tfrac{1}{2}\gamma_e - \tfrac{1}{2}\gamma_i\right) \\ &\quad + 2C_\Gamma\left(\dot{\tilde{\Gamma}}_i - \dot{\tilde{\Gamma}}_e + \tfrac{1}{2}\dot{\gamma}_e - \tfrac{1}{2}\dot{\gamma}_i\right) - 2[K_\Gamma - H_e(\dot{\tilde{\Phi}}_e)](\tilde{\Gamma}_i - \tilde{\Gamma}_e) \\ &\quad = [K_\Gamma - H_e(\dot{\tilde{\Phi}}_e)](\gamma_e - \gamma_i) + 2C_\Gamma(\dot{\tilde{\Gamma}}_i - \dot{\tilde{\Gamma}}_e) + C_\Gamma(\dot{\gamma}_e - \dot{\gamma}_i) \\ &\quad \cong \mathcal{P}(\tilde{\Phi}_e)\boldsymbol{w}_p + 2C_\Gamma(\dot{\tilde{\Gamma}}_i - \dot{\tilde{\Gamma}}_e) \end{aligned} \tag{79}$$

where

$$\mathcal{P}(\tilde{\Phi}_e) = k_t \begin{pmatrix} \cos\tilde{\theta}_e & -\sin\tilde{\theta}_e & 0 \\ \sin\tilde{\theta}_e & \cos\tilde{\theta}_e & 0 \\ 0 & 0 & 1 \end{pmatrix} \tag{80}$$

Finally, defining by $\mathcal{S}_i$ and $\mathcal{S}_e$ the two-column matrices such that

$$\frac{J_{t_i}}{\chi_i \omega_s^2\left(J_{t_i} - J_{p_i}\right)}\mathcal{S}_i = \frac{J_{t_e}}{\chi_e \omega_s^2\left(J_{t_e} - J_{p_e}\right)}\mathcal{S}_e = \begin{pmatrix} 0 & -1 \\ 1 & 0 \\ 0 & 0 \end{pmatrix} \tag{81}$$

we obtain a system of the form

$$\begin{aligned} m_i\ddot{\tilde{\Gamma}}_i &= -\mathcal{G}_i(\tilde{\Gamma}_i)\tilde{\Gamma}_i - 2[K_\Gamma - H_i(\dot{\tilde{\Phi}}_i)](\tilde{\Gamma}_i - \tilde{\Gamma}_e) \\ &\quad - 2C_\Gamma(\dot{\tilde{\Gamma}}_i - \dot{\tilde{\Gamma}}_e) + \boldsymbol{u}_{\Gamma_i} - \mathcal{P}(\tilde{\Phi}_e)\boldsymbol{w}_p + \mathcal{A}_i(\tilde{\Gamma}_i)\boldsymbol{w}_o \end{aligned} \tag{82}$$

$$\begin{aligned} \ddot{\tilde{\Phi}}_i &= -\Lambda_i(\dot{\tilde{\Phi}}_i)(\dot{\tilde{\Phi}}_i + \mathbf{Y}) + 2\Sigma_i[-K_\Phi(\tilde{\Phi}_i - \tilde{\Phi}_e) \\ &\quad - C_\Phi(\dot{\tilde{\Phi}}_i - \dot{\tilde{\Phi}}_e)] + \mathcal{S}_i\boldsymbol{w}_s \end{aligned} \tag{83}$$

$$\begin{aligned} m_e\ddot{\tilde{\Gamma}}_e &= -\mathcal{G}_e(\tilde{\Gamma}_e)\tilde{\Gamma}_e + 2[K_\Gamma - H_e(\dot{\tilde{\Phi}}_e)](\tilde{\Gamma}_i - \tilde{\Gamma}_e) + 2C_\Gamma(\dot{\tilde{\Gamma}}_e - \dot{\tilde{\Gamma}}_i) \\ &\quad - \boldsymbol{u}_{\Gamma_i} + \boldsymbol{u}_{\Gamma_e} + \mathcal{P}(\tilde{\Phi}_e)\boldsymbol{w}_p + \mathcal{D}\boldsymbol{w}_d + \mathcal{A}_e(\tilde{\Gamma}_e)\boldsymbol{w}_o \end{aligned} \tag{84}$$

$$\begin{aligned} \ddot{\tilde{\Phi}}_e &= -\Lambda_e(\dot{\tilde{\Phi}}_e)(\dot{\tilde{\Phi}}_e + \mathbf{Y}) + 2\Sigma_e[K_\Phi(\tilde{\Phi}_i - \tilde{\Phi}_e) \\ &\quad + C_\Phi(\dot{\tilde{\Phi}}_i - \dot{\tilde{\Phi}}_e)] + \mathcal{S}_e\boldsymbol{w}_s \end{aligned} \tag{85}$$

where

$$\mathcal{A}_i(\tilde{\Gamma}_i) = \mathcal{H} - \mathcal{F}_i(\tilde{\Gamma}_i) \tag{86}$$

$$\mathcal{A}_e(\tilde{\Gamma}_e) = \mathcal{H} - \mathcal{F}_e(\tilde{\Gamma}_e) \tag{87}$$

Grouping the vectors introduced as

$$\tilde{\boldsymbol{x}} = \begin{pmatrix} \tilde{\Gamma}_i \\ \tilde{\Phi}_i \\ \tilde{\Gamma}_e \\ \tilde{\Phi}_e \\ \dot{\tilde{\Gamma}}_i \\ \dot{\tilde{\Phi}}_i \\ \dot{\tilde{\Gamma}}_e \\ \dot{\tilde{\Phi}}_e \end{pmatrix} \qquad \boldsymbol{u} = \begin{pmatrix} \boldsymbol{u}_{\Gamma_i} \\ \boldsymbol{u}_{\Gamma_e} \end{pmatrix} \qquad \boldsymbol{w} = \begin{pmatrix} w_p \\ w_d \\ w_s \\ w_o \end{pmatrix} \tag{88}$$

we obtain the compact form

$$\dot{\tilde{\boldsymbol{x}}} = \tilde{f}(\tilde{\boldsymbol{x}}) + g(\tilde{\boldsymbol{x}})\boldsymbol{u} + \tilde{p}(\tilde{\boldsymbol{x}})\boldsymbol{w} \tag{89}$$

$$\tilde{\boldsymbol{y}} = h(\tilde{\boldsymbol{x}}) \tag{90}$$

[note that the choice of $\boldsymbol{q}(\boldsymbol{x}) = 0$ means that a desired output

$$\tilde{\Gamma}_i = 0 \qquad \tilde{\Gamma}_e = 0$$

is required, and both the cylinders must track the orbit], namely,

$$\begin{aligned} \dot{\tilde{\boldsymbol{x}}} = &\underbrace{\begin{pmatrix} \tilde{\Gamma}_i \\ \tilde{\Phi}_i \\ \tilde{\Gamma}_e \\ \tilde{\Phi}_e \\ m_i^{-1}[-\mathcal{G}_i(\tilde{\Gamma}_i)\tilde{\Gamma}_i - 2[K_\Gamma - H_i(\dot{\tilde{\Phi}}_i)](\tilde{\Gamma}_i - \tilde{\Gamma}_e) - 2C_\Gamma(\dot{\tilde{\Gamma}}_i - \dot{\tilde{\Gamma}}_e)] \\ -\Lambda_i(\dot{\tilde{\Phi}}_i)(\dot{\tilde{\Phi}}_i + \mathbf{Y}) - 2\Sigma_i[K_\Phi(\tilde{\Phi}_i - \tilde{\Phi}_e) + C_\Phi(\dot{\tilde{\Phi}}_i - \dot{\tilde{\Phi}}_e)] \\ m_e^{-1}\{-\mathcal{G}_e(\tilde{\Gamma}_e)\tilde{\Gamma}_e + 2[K_\Gamma - H_e(\dot{\tilde{\Phi}}_e)](\tilde{\Gamma}_i - \tilde{\Gamma}_e) + 2C_\Gamma(\dot{\tilde{\Gamma}}_e - \dot{\tilde{\Gamma}}_i)\} \\ -\Lambda_e(\dot{\tilde{\Phi}}_e)(\dot{\tilde{\Phi}}_e + \mathbf{Y}) + 2\Sigma_e[K_\Phi(\tilde{\Phi}_i - \tilde{\Phi}_e) + C_\Phi(\dot{\tilde{\Phi}}_i - \dot{\tilde{\Phi}}_e)] \end{pmatrix}}_{\tilde{f}(\tilde{x})} + \underbrace{\begin{pmatrix} 0 & 0 \\ 0 & 0 \\ 0 & 0 \\ 0 & 0 \\ \left[B_{11}^i\right]^{-1} & 0 \\ 0 & 0 \\ -\left[B_{11}^e\right]^{-1} & \left[B_{11}^e\right]^{-1} \\ 0 & 0 \end{pmatrix}}_{g(\tilde{x})}\boldsymbol{u} \\ &+ \underbrace{\begin{pmatrix} 0 & 0 & 0 & 0 \\ 0 & 0 & 0 & 0 \\ 0 & 0 & 0 & 0 \\ 0 & 0 & 0 & 0 \\ -(1/m_i)\mathcal{P}(\tilde{\Phi}_e) & 0 & 0 & \mathcal{A}_i(\tilde{\Gamma}_i) \\ 0 & 0 & \mathcal{S}_i & 0 \\ (1/m_e)\mathcal{P}(\tilde{\Phi}_e) & (1/m_e)\mathcal{D} & 0 & \mathcal{A}_e(\tilde{\Gamma}_e) \\ 0 & 0 & \mathcal{S}_e & 0 \end{pmatrix}}_{\tilde{p}(\tilde{x})}\boldsymbol{w} \end{aligned} \tag{91}$$

$$\tilde{y} = y(\tilde{x}) = \begin{pmatrix} \tilde{\Gamma}_i - \tilde{\Gamma}_e \\ \tilde{\Gamma}_e \end{pmatrix} \tag{92}$$

In this way we have obtained Eqs. (41) and (43) of the standard form, where $f(0) = 0$ and $h(0) = 0$. [In particular, $f(0) = 0$ in the rotational equations follows from that $x = 0$ implies $\tilde{\Phi}_i = \tilde{\Phi}_e = \dot{\tilde{\Phi}}_i = \dot{\tilde{\Phi}}_e$ and $\Lambda_i(\dot{\tilde{\Phi}}_i)\mathbf{Y} = \Lambda_e(\dot{\tilde{\Phi}}_e)\mathbf{Y} = 0$.]

Computation of the Control Law

The controller we are looking for is an output regulation control law via error feedback under parameter uncertainties. The uncertainties are considered as components of an augmented exogenous input generated by the augmented exosystem. The main difference between this approach and traditional regulation frameworks is the possibility to include in the exogenous input w also the parameters $\epsilon_{xe}, \epsilon_{x_i}, \epsilon_{y_i}, \epsilon_{ye}, \epsilon_{z_i}$, and ϵ_{ze}.

With this in mind the computation of the exosystem can be performed as follows.

The perturbations are assumed to be generated by

$$\dot{w}_p = S_p w_p = \begin{pmatrix} 0 & -\omega_s & 0 \\ \omega_s & 0 & 0 \\ 0 & 0 & 0 \end{pmatrix} w_p \tag{93}$$

The drag forces are assumed to be generated by

$$\dot{w}_d = S_d w_d = \begin{pmatrix} 0 & -\omega_o & 0 & 0 \\ \omega_o & 0 & 0 & 0 \\ 0 & 0 & 0 & -2\omega_o \\ 0 & 0 & 2\omega_o & 0 \end{pmatrix} w_d \tag{94}$$

Also w_s and w_o are assumed to be generated by

$$\dot{w}_s = S_s w_s = \begin{pmatrix} 0 & -\omega_s \\ \omega_s & 0 \end{pmatrix} w_s \tag{95}$$

$$\dot{w}_o = S_o w_o = \begin{pmatrix} 0 & -\omega_o & 0 & 0 & 0 \\ \omega_o & 0 & 0 & 0 & 0 \\ 0 & 0 & 0 & \omega_o & -\omega_o \\ 0 & 0 & -2\omega_o & 0 & 0 \\ 0 & 0 & 2\omega_o & 0 & 0 \end{pmatrix} w_o \tag{96}$$

So that the exosystem can be represented by the linear equation

$$\dot{w} = Sw = \begin{pmatrix} S_p & & & 0 \\ & S_d & & \\ & & S_s & \\ 0 & & & S_o \end{pmatrix} w \tag{97}$$

As far as the detectability and stabilizability conditions (Hypotheses 2 and 3) are concerned, we note that the linear approximation (44) of the system takes the form

$$\dot{\tilde{x}} = A\tilde{x} + Bu + Pw \tag{98}$$

$$\tilde{y} = C\tilde{x} \tag{99}$$

where

$$A = \begin{pmatrix} 0 & 0 & 0 & 0 & I_3 & 0 & 0 & 0 \\ 0 & 0 & 0 & 0 & 0 & I_3 & 0 & 0 \\ 0 & 0 & 0 & 0 & 0 & 0 & I_3 & 0 \\ 0 & 0 & 0 & 0 & 0 & 0 & 0 & I_3 \\ A_{51} & 0 & A_{53} & 0 & A_{55} & 0 & A_{57} & 0 \\ 0 & A_{62} & 0 & A_{62} & 0 & A_{66} & 0 & A_{68} \\ A_{71} & 0 & A_{73} & 0 & A_{75} & 0 & A_{77} & 0 \\ 0 & A_{82} & 0 & A_{84} & 0 & A_{86} & 0 & A_{88} \end{pmatrix} \tag{100}$$

$$B = \begin{pmatrix} 0 & 0 \\ 0 & 0 \\ 0 & 0 \\ 0 & 0 \\ B_{11}^{i^{-1}} & 0 \\ 0 & 0 \\ -B_{11}^{e^{-1}} & B_{11}^{e^{-1}} \\ 0 & 0 \end{pmatrix} \qquad P = \begin{pmatrix} 0 & 0 & 0 & 0 \\ 0 & 0 & 0 & 0 \\ 0 & 0 & 0 & 0 \\ 0 & 0 & 0 & 0 \\ -(1/m_1)\mathcal{P}_0 & 0 & 0 & 0 \\ 0 & 0 & \mathcal{S}_i & 0 \\ (1/m_e)\mathcal{P}_0 & (1/m_e)\mathcal{D} & 0 & 0 \\ 0 & 0 & \mathcal{S}_e & 0 \end{pmatrix} \tag{101}$$

$$C = \begin{pmatrix} I_3 & 0 & -I_3 & 0 & 0 & 0 & 0 & 0 \\ 0 & 0 & I_3 & 0 & 0 & 0 & 0 & 0 \end{pmatrix} \qquad Q = 0_{6\times 16} \tag{102}$$

(In particular, $P_{54} = P_{74} = 0$ arises from the third law of Kepler

$$R^3 \big/ T_0^2 = G_u m_\oplus \big/ 4\pi^2$$

where

$$T_0 = 2\pi/\omega_o$$

is the orbital period, about 1 h, 35 min.)

From Eqs. (100–102) it follows that only the translational dynamics are controllable by the inputs u_{Γ_i} and u_{Γ_e}. This means that the system is stabilizable, because the uncontrollable (rotational) dynamics are stable. Hence, in suitable coordinates, $z = Tx$, A and B take the form

$$\tilde{A} = TAT^{-1} = \begin{pmatrix} \tilde{A}_{11} & 0 \\ 0 & \tilde{A}_{22} \end{pmatrix} \qquad \tilde{B} = TB = \begin{pmatrix} \tilde{B}_1 \\ 0 \end{pmatrix} \tag{103}$$

with $\sigma(\tilde{A}_{22}) \subset \mathbb{C}^-$ and

$$K = (\tilde{K}_1 \quad 0)T \qquad \tilde{K}_1 : \sigma(\tilde{A}_{11} + \tilde{B}_1\tilde{K}_1) \subset \mathbb{C}^- \tag{104}$$

The pair (C_e, A_e) is stabilizable because the translational dynamics are fully observable, whereas the unobservable ones are stable. Hence, in suitable coordinates $\zeta = Ux$, A_e and C_e take the form

$$\tilde{A}_e = UA_eU^{-1} = \begin{pmatrix} \tilde{A}'_{11} & 0 \\ 0 & \tilde{A}'_{22} \end{pmatrix} \qquad \tilde{C}_e = C_eU^{-1} = (\tilde{C}_1 \quad 0) \tag{105}$$

with $\sigma(\tilde{A}'_{22}) \subset \mathbb{C}^-$ and

$$G = U^{-1}\begin{pmatrix} 0 \\ \tilde{G}_2 \end{pmatrix} \qquad \tilde{G}_2 : \sigma(\tilde{A}'_{11} - \tilde{G}_2\tilde{C}_1) \subset \mathbb{C}^- \tag{106}$$

The state feedback controller and the error feedback controller can now be computed by solving Eqs. (57) and (58) obtaining

$$\pi(w) = \begin{pmatrix} \pi_{\tilde{\Gamma}_i} \\ \pi_{\tilde{\Phi}_i} \\ \pi_{\tilde{\Gamma}_e} \\ \pi_{\tilde{\Phi}_e} \\ \pi_{\dot{\tilde{\Gamma}}_i} \\ \pi_{\dot{\tilde{\Phi}}_i} \\ \pi_{\dot{\tilde{\Gamma}}_e} \\ \pi_{\dot{\tilde{\Phi}}_e} \end{pmatrix} \qquad c(w) = Lw \tag{107}$$

where

$$\pi_{\tilde{\Gamma}_i} = \pi_{\tilde{\Gamma}_e} = \pi_{\dot{\tilde{\Gamma}}_i} = \pi_{\dot{\tilde{\Gamma}}_e} = \begin{pmatrix} 0 \\ 0 \\ 0 \end{pmatrix} \tag{108}$$

$$\frac{\pi_{\tilde{\Phi}_i}}{\chi_i} = \frac{\pi_{\tilde{\Phi}_e}}{\chi_e} = \begin{pmatrix} w_y^s \\ -w_x^s \\ 0 \end{pmatrix} \tag{109}$$

$$\frac{\pi_{\dot{\tilde{\Phi}}_i}}{\chi_i} = \frac{\pi_{\dot{\tilde{\Phi}}_e}}{\chi_e} = \omega_s \begin{pmatrix} w_x^s \\ w_y^s \\ 0 \end{pmatrix} \tag{110}$$

$$L = \begin{pmatrix} \mathcal{P}_0 & 0 & 0 & 0 \\ 0 & -\mathcal{D} & 0 & 0 \end{pmatrix} \tag{111}$$

$$\mathcal{P}_o = \mathcal{P}(\tilde{\Phi}_e)|_{\tilde{\theta}_e = 0} = \begin{pmatrix} k_t & 0 & 0 \\ 0 & k_t & 0 \\ 0 & 0 & k_t \end{pmatrix} \tag{112}$$

More details about the development of these solutions can be found in Appendix D.

Based on the foregoing development, we can conclude that the state feedback control action computed by solving the regulation Eqs. (57) and (58) takes the form

$$\boldsymbol{u} = K\tilde{\boldsymbol{x}} + L\boldsymbol{w} \tag{113}$$

which is linear in $\tilde{\boldsymbol{x}}$ and $\boldsymbol{w}$ [$c(\boldsymbol{w})$ is linear and $K\pi(\boldsymbol{w}) = 0$ in Eq. (50)] in spite of the nonlinearity of Eqs. (57) and (58). [It has been assumed that

$$K[\tilde{x} - \pi(w)] = K\tilde{x}$$

because of the uncontrollability of the rotational dynamics, which determines the following structure for K: $K = (K_1\ 0\ K_2\ 0\ K_3\ 0\ K_4\ 0)$].

The error feedback controller (59–61) takes the nonlinear form

$$\dot{\xi}_1 = \tilde{f}(\xi_1) + \tilde{p}(\xi_1)\xi_2 + g(\xi_1)(K\xi_1 + L\xi_2) - G_1\left[\begin{pmatrix} \xi_{\tilde{\Gamma}_i} - \xi_{\tilde{\Gamma}_e} \\ \xi_{\tilde{\Gamma}_e} \end{pmatrix} - \begin{pmatrix} \tilde{\Gamma}_i - \tilde{\Gamma}_e \\ \tilde{\Gamma}_e \end{pmatrix}\right] \tag{114}$$

$$\dot{\xi}_2 = S\xi_2 - G_2\left[\begin{pmatrix} \xi_{\tilde{\Gamma}_i} - \xi_{\tilde{\Gamma}_e} \\ \xi_{\tilde{\Gamma}_e} \end{pmatrix} - \begin{pmatrix} \tilde{\Gamma}_i - \tilde{\Gamma}_e \\ \tilde{\Gamma}_e \end{pmatrix}\right] \tag{115}$$

$$\theta(\xi_1, \xi_2) = K\xi_1 + L\xi_2 \tag{116}$$

where

$$\xi_1 = \begin{pmatrix} \xi_{\tilde{\Gamma}_i} \\ \xi_{\tilde{\Phi}_i} \\ \xi_{\tilde{\Gamma}_e} \\ \xi_{\tilde{\Phi}_e} \\ \xi_{\dot{\tilde{\Gamma}}_i} \\ \xi_{\dot{\tilde{\Phi}}_i} \\ \xi_{\dot{\tilde{\Gamma}}_e} \\ \xi_{\dot{\tilde{\Phi}}_e} \end{pmatrix} \qquad \xi_2 = \begin{pmatrix} \xi_p \\ \xi_d \\ \xi_s \\ \xi_o \end{pmatrix} \tag{117}$$

Simulation Results

Several simulations have been performed using the error feedback controller (114–116) on the simulation model, and the results are briefly discussed in this section. The numerical values of the parameters used are reported in Table 1.

In all of the simulations to be discussed the matrices K and G are fixed to set time constants τ_i to 1 s where the PGB–S/C configuration has been considered ($m_i = m_{\mathrm{PGB}}$, $m_e = m_{\mathrm{S/C}}$, $J_{p_i} = J_{p\,\mathrm{PGB}}$, $J_{p_e} = J_{p\,\mathrm{S/C}}$, $J_{t_i} = J_{t\,\mathrm{PGB}}$, and $J_{t_e} = J_{t\,\mathrm{S/C}}$). Three different cases have been considered to show the feasibility of the controller with respect to the strong constraints on the control values ($\|\boldsymbol{u}_{\Gamma_i}\| < 10^{-4}$ N, $\|\boldsymbol{u}_{\Gamma e}\| < 10^{-4}$ N), the effectiveness of the regulation in presence of variations of measures and modeled disturbances and the robustness of the controller with respect to parameters variation.

The results of the first simulation are in Figs. 2–5. Figure 2 shows the xy relative displacement between masses, namely, $\sqrt{[(\tilde{x}_i - \tilde{x}_e)^2 + (\tilde{y}_i - \tilde{y}_e)^2]}$. Figure 3 shows the behavior of $\sqrt{(\tilde{x}_e^2 + \tilde{y}_e^2)}$, the xy tracking error along the nominal orbital trajectory. Figures 4 and 5 show the control action provided by the AD and FEEP thrusters.

Table 1 Numerical values of the parameters

Parameter	Value
Process parameters	
m_{PGB}	43.7 kg
$J_{p\,\mathrm{PGB}}$	3.2 kg m^2
$J_{t\,\mathrm{PGB}}$	2.2 kg m^2
$m_{\mathrm{S/C}}$	122.1 kg
$J_{p\,\mathrm{S/C}}$	29.2 kg m^2
$J_{t\,\mathrm{S/C}}$	19.6 kg m^2
$m_{\mathrm{TM}_i} = m_{\mathrm{TM}_e}$	10.0 kg
$J_{p\,\mathrm{TM}_i} = J_{p\,\mathrm{TM}_e}$	0.0752 kg m^2
$J_{t\,\mathrm{TM}_i} = J_{t\,\mathrm{TM}_e}$	0.0754 kg m^2
χ_i and χ_e	0.1 deg
k_t	0.01 kg s^{-2}
c_t	1.6×10^{-5} kg s^{-1}
Controller parameters	
τ_i	1 s (for nonlinear regulation)
k_d	0.5 Ns/m (for derivative controller)
Simulation parameters	
T_0	$\cong$ 1 h 35 mm
ω_s	2 Hz
ω_o	1.75×10^{-4} Hz
$\epsilon_{x_e} - \epsilon_{x_i}$	10 μm
$\epsilon_{y_e} - \epsilon_{y_i}$	6 μm
$\epsilon_{z_e} - \epsilon_{z_i}$	14 μm
R	6898 km
d_1	7.12×10^{-6} N
d_2	2.81×10^{-6} N

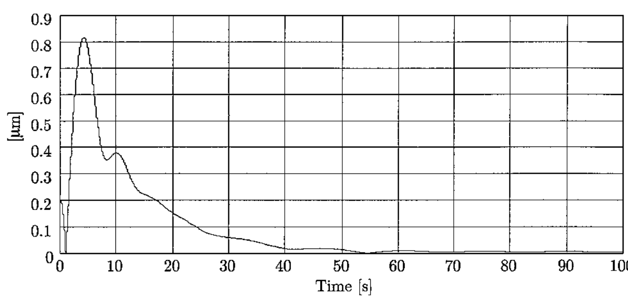

Fig. 2 Relative displacement between cylinders.

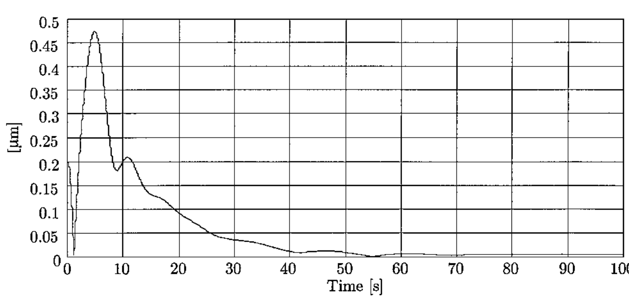

Fig. 3 Case 1: orbit tracking error.

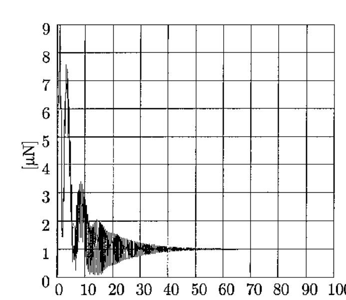

Fig. 4 Case 1: AD thrust.

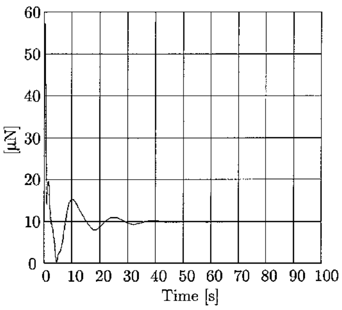

Fig. 5 Case 1: FEEP thrust.

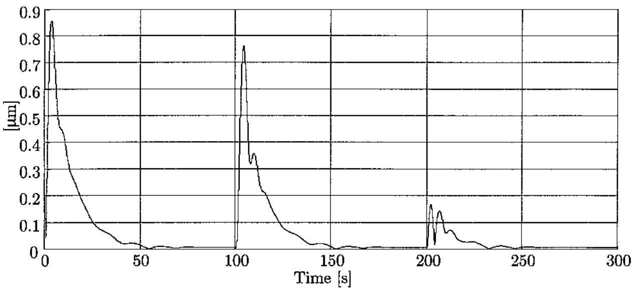

Fig. 6 Case 2: relative displacement between cylinders.

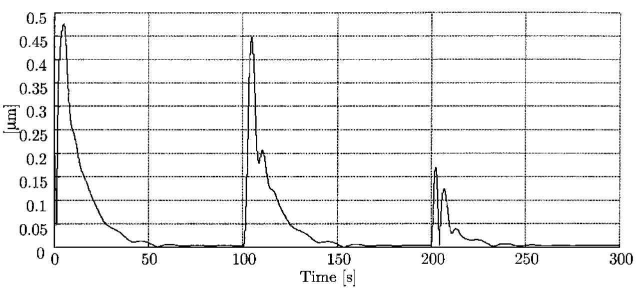

Fig. 7 Case 2: orbit tracking error.

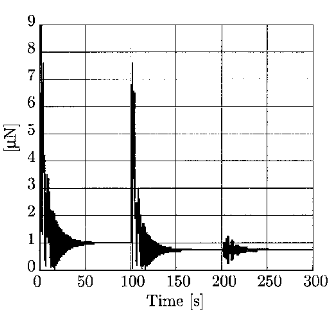

Fig. 8 Case 2: AD thrust.

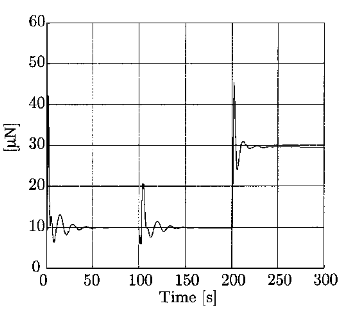

Fig. 9 Case 2: FEEP thrust.

In particular, this is evident because during steady state the FEEP thrusters balance the drag force ($\cong d_1 + d_2 \cong 9.93 \times 10^{-6}$ N in the early seconds) within an error of about 10^{-10} N.

The efficiency of the controller with respect to an initial condition mismatch is shown by the results of the second simulation (Figs. 6–9). During the simulation, a state mismatch at $t = 0$ (within 20% around) is assumed, together with a switching of the amplitude of w_p and $\boldsymbol{w}_d$ (occurring at $t = 100$ s and $t = 200$ s, respectively).

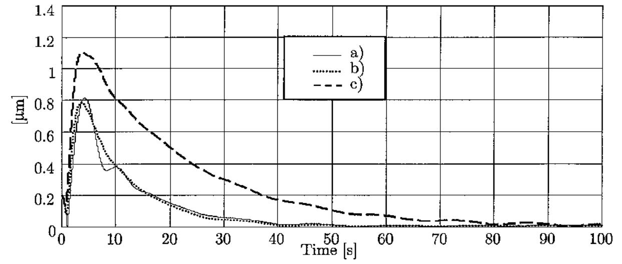

Fig. 10 Case 3: relative displacement between cylinders.

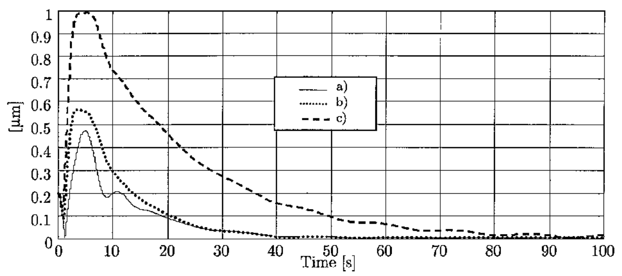

Fig. 11 Case 3: orbit tracking error.

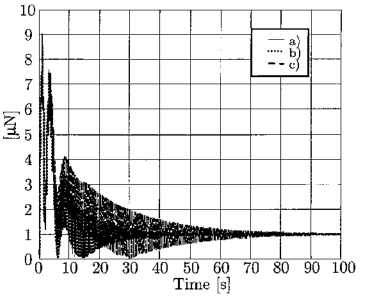

Fig. 12 Case 3: AD thrust.

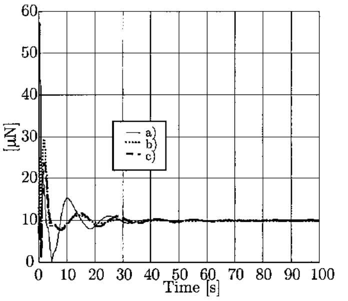

Fig. 13 Case 3: FEEP thrust.

The results of a third simulation are in Figs. 10–13. Here, some nonestimated parameters have been changed from their nominal values to verify the robustness of the controller. In particular the analysis has been developed with respect to mass variations, the most critical parameter. More precisely, line a represents the nominal situation where the real values for the masses, for example, m_i^0 and m_e^0, have been assumed; line b shows the behavior by assuming $m_i = 2m_i^0$ and $m_e = 0.5m_e^0$; and line c shows the behavior by assuming $m_i = 4m_i^0$ and $m_e = 0.25m_e^0$.

Table 2 reports in synthesis the results of a comparative analysis between nonlinear regulation and the controller proposed in Refs. 3 and 6 for achieving stabilization of the whirling modes, where a control action of the form

$$\boldsymbol{u}_{\Gamma_i} = -k_d \frac{\mathrm{d}}{\mathrm{d}t}(2\tilde{\Gamma}_i - 2\tilde{\Gamma}_e - \gamma_i + \gamma_e) \tag{118}$$

$$\boldsymbol{u}_{\Gamma_e} = \boldsymbol{d}_c(t) \tag{119}$$

is used, which means a derivative controller plus an open-loop direct compensation of the atmospheric drag. When the numeric values in Table 2 are examined, the effectiveness of the proposed controller is evident in terms of high-precision tracking (very small $\Delta\tilde{c}$) vs increased power consumption (higher values of AD thrust).

The second column of Table 2 and Fig. 14 evidence the degraded behavior of the control system under the action of the derivative controller tuned up providing a comparable thrust amplitude. In particular, it is evident that the transient behavior increases up to 7300 s.

Finally, note the possibility of detecting a violation of the EP under the action of the proposed controller. Because an eventual violation would result in a perturbation rejected by the controller,

Table 2 Numerical results of the performed comparative simulations

	Derivative[a]		Nonlinear regulation
Parameter	$k_d = 0.5$	$k_d = 0.0206$	$\tau_i = 1$
$t_{0.1}$, s	506	7,300	39
Δc^*, μm	1.16	1.16	1.16
$\Delta\tilde{c}$, μm	0.025	0.014	0.001
T^*_{AD}, μN	73.1	3	9
$\tilde{T}_{\mathrm{AD}}$, μN	72.9	3	1
$\hat{E}_{\mathrm{AD}}$, μN·s	14,583	599	227
$\tilde{E}_{\mathrm{AD}}$, μN·s	14,560	600	200
T^*_{FEEP}, μN	10.03	10.03	57
$\tilde{T}_{\mathrm{FEEP}}$, μN	10.03	10.03	9.93
$\hat{E}_{\mathrm{FEEP}}$, μN·s	2,006	2,006	2,504
$\tilde{E}_{\mathrm{FEEP}}$, μN·s	2,006	2,006	1,968

[a]Drag compensation error of 1% assumed.

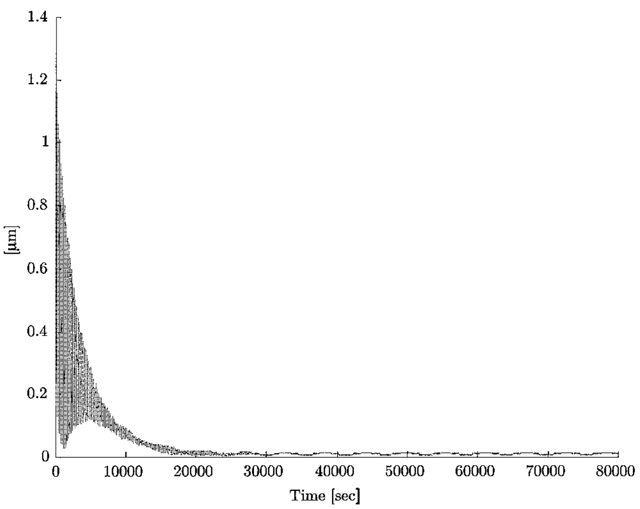

Fig. 14 Derivative controller: relative displacement between cylinders.

it has been planned that the experimental phase be during uncontrolled evolutions of the satellite. Thus, controlled evolution should alternate to free motion periods to perform the needed measures. A different approach, suggested by intuition, refers to the possibility of detecting the EP violation from the analysis of the control signal, evidencing a variation of its amplitude at orbital frequency.

This approach has been simulated to verify the effectiveness of such a solution. The TM configuration has been used ($m_i = m_{\mathrm{TM}_i}$, $m_e = m_{\mathrm{TM}_e}$, $J_{pi} = J_{p\mathrm{TM}_i}$, $J_{pe} = J_{p\mathrm{TM}_e}$, $J_{ti} = J_{t\mathrm{TM}_i}$ and $J_{te} = J_{t\mathrm{TM}_e}$), and a violation of about 10^{-16} m/s^2 has been introduced. In Fig. 15 the fast Fourier transform (FFT) magnitude of the active dampers control signal components are shown. The different values at ω_o frequency reveal the presence of the simulated EP violation.

Conclusions

The nonlinear regulation approach has been applied to solve the problem of achieving exact orbit tracking and asymptotic drag compensation for a two bodies spinning satellite in LEO. The particular case of Galileo Galilei mission, where the stabilization of the whirling modes assumes a fundamental role, has been examined. The results of the simulations show the effectiveness of the proposed controller.

The same control scheme can be applied to stabilize the inner bodies, that is, the test masses of the experiment in the more complex (four bodies) mechanical structure employed in the Galileo Galilei experiment. In this case, drag forces do not act, and only electrostatic dampers are available.

The possibility of detecting a violation of the EP from the analysis of the control signal is also evidenced and validated by a simulation.

Appendix A: Terms in Equations (14) and (15)

The expression of matrices B^i_{11}, B^e_{11}, $B^i_{22}(\Phi_i)$ and $B^e_{22}(\Phi_e)$ in Eqs. (14) and (15) are

$$B^i_{11} = \begin{pmatrix} m_i & 0 & 0 \\ 0 & m_i & 0 \\ 0 & 0 & m_i \end{pmatrix} \qquad B^e_{11} = \begin{pmatrix} m_e & 0 & 0 \\ 0 & m_e & 0 \\ 0 & 0 & m_e \end{pmatrix} \tag{A1}$$

$$B^i_{22}(\Phi_i) = B_{22}(\Phi)|_{\Phi=\Phi_i} \tag{A2}$$

$$B^e_{22}(\Phi_e) = B_{22}(\Phi)|_{\Phi=\Phi_e} \tag{A3}$$

where

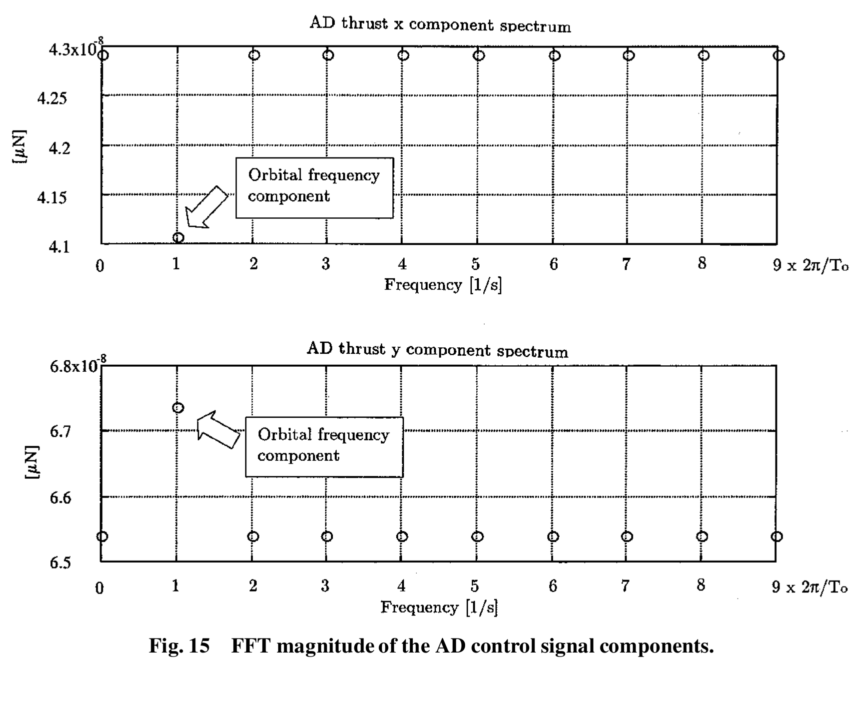

Fig. 15 FFT magnitude of the AD control signal components.

$$
B_{22}(\Phi)=\begin{pmatrix}
\begin{array}{c} J_p\cos^2\chi\sin^2\psi \\ +J_p\sin^2\chi\cos^2\theta\cos^2\psi \\ +J_t\sin^2\theta\cos^2\psi \\ +J_t\sin^2\chi\sin^2\psi \\ +J_t\cos^2\chi\cos^2\theta\cos^2\psi \\ +\frac{1}{2}J_p\cos\theta\sin 2\chi\sin 2\psi \\ -\frac{1}{2}J_t\cos\theta\sin 2\chi\sin 2\psi \end{array} &
\begin{array}{c} \frac{1}{2}J_p\sin^2\chi\cos\psi\sin 2\theta \\ -\frac{1}{2}J_t\sin 2\chi\sin\psi\sin\theta \\ -\frac{1}{2}J_t\sin 2\theta\cos\psi \\ +\frac{1}{2}J_p\sin 2\chi\sin\psi\sin\theta \\ +\frac{1}{2}J_t\cos^2\chi\cos\psi\sin 2\theta \end{array} &
\begin{array}{c} J_p\cos^2\chi\sin\psi \\ +J_t\sin^2\chi\sin\psi \\ +\frac{1}{2}J_p\cos\theta\cos\psi\sin 2\chi \\ -\frac{1}{2}J_t\cos\theta\cos\psi\sin 2\chi \end{array} \\
* & \begin{array}{c} J_t\cos^2\chi\sin^2\theta \\ +J_p\sin^2\chi\sin^2\theta \\ +J_t\cos^2\theta \end{array} & \begin{array}{c} J_p\cos\chi\sin\theta\sin\chi \\ -J_t\cos\chi\sin\theta\sin\chi \end{array} \\
* & * & J_t\sin^2\chi+J_p\cos^2\chi
\end{pmatrix}
\tag{A4}
$$

and

$$C^i_{22}(\Phi_i)=C_{22}(\Phi)|_{\Phi=\Phi_i} \tag{A5}$$

$$C^e_{22}(\Phi_e)=C_{22}(\Phi)|_{\Phi=\Phi_e} \tag{A6}$$

where

The matrices $G^i_{11}(\Gamma)$ and $G^e_{11}(\Gamma_e)$ in Eqs. (14) and (15) are given by

$$
G^i_{11}(\Gamma_i)=\frac{G_u m_\oplus m_i}{\sqrt{x_i^2+y_i^2+z_i^2}}\begin{pmatrix}1&0&0\\0&1&0\\0&0&1\end{pmatrix} \tag{A8}
$$

$$
C_{22}(\Phi)=\begin{pmatrix}
\begin{array}{c} 2J_p\cos\theta\cos^2\psi\sin 2\chi\dot\psi \\ -J_t\cos^2\chi\cos^2\psi\sin 2\theta\dot\theta \\ -J_t\cos^2\chi\cos^2\theta\sin 2\psi\dot\psi \\ -J_p\cos^2\theta\sin 2\psi\dot\psi \\ -2J_t\cos\theta\cos^2\psi\sin 2\chi\dot\psi \\ +J_p\cos^2\psi\sin 2\theta\dot\theta\cos^2\chi \\ +J_t\sin 2\psi\dot\psi\cos^2\theta \\ +J_p\cos^2\theta\sin 2\psi\dot\psi\cos^2\chi \\ +\frac{1}{2}J_t\sin\theta\dot\theta\sin 2\chi\sin 2\psi \\ +J_p\cos^2\chi\sin 2\psi\dot\psi \\ -J_t\sin 2\psi\dot\psi\cos^2\chi \\ -J_p\cos^2\psi\sin 2\theta\dot\theta \\ +J_t\sin 2\theta\cos^2\psi\dot\theta \\ -J_p\cos\theta\dot\psi\sin 2\chi \\ -\frac{1}{2}J_p\sin\theta\dot\theta\sin 2\chi\sin 2\psi \\ +J_t\cos\theta\dot\psi\sin 2\chi \end{array} &
\begin{array}{c} -J_p\dot\theta\cos\psi \\ +J_p\cos\theta\sin\psi\sin 2\chi\dot\theta \\ +2J_t\cos^2\chi\cos^2\theta\cos\psi\dot\theta \\ -2J_t\cos^2\theta\dot\theta\cos\psi \\ +2J_p\dot\theta\cos\psi\cos^2\theta \\ -2J_p\dot\theta\cos\psi\cos^2\chi\cos^2\theta \\ -J_t\cos\theta\sin\psi\sin 2\chi\dot\theta \\ -J_p\dot\phi\cos^2\chi\sin\psi\cos\psi \\ -J_p\dot\phi\cos\theta\cos^2\psi\sin 2\chi \\ +J_t\dot\phi\cos\theta\cos^2\psi\sin 2\chi \\ +\frac{1}{2}J_t\dot\phi\cos^2\chi\cos^2\theta\sin 2\psi \\ -J_t\dot\phi\cos\chi\cos\theta\sin\chi \\ +J_p\dot\phi\cos^2\theta\cos\psi\sin\psi \\ +J_p\dot\phi\cos\chi\cos\theta\sin\chi \\ -J_t\dot\phi\sin\psi\cos\psi\cos^2\theta \\ +J_t\dot\phi\sin\psi\cos\psi\cos^2\chi \\ -\frac{1}{2}J_p\dot\phi\cos^2\theta\sin 2\psi\cos^2\chi \end{array} &
\begin{array}{c} 2J_p\cos^2\theta\cos\psi\dot\psi\cos^2\chi \\ +J_t\sin 2\chi\sin\psi\cos\theta\dot\psi \\ +J_p\cos\psi\dot\psi \\ -J_p\sin 2\chi\sin\psi\cos\theta\dot\psi \\ -2J_p\cos^2\theta\cos\psi\dot\psi \\ +2J_t\cos^2\theta\cos\psi\dot\psi \\ -2J_t\cos^2\chi\cos^2\theta\cos\psi\dot\psi \\ -\frac{1}{2}J_p\dot\phi\cos^2\psi\sin 2\theta\cos^2\chi \\ +J_p\dot\phi\cos\theta\cos^2\psi\sin\theta \\ -J_t\sin\theta\cos^2\psi\dot\phi\cos\theta \\ -\frac{1}{4}J_t\dot\phi\sin\theta\sin 2\chi\sin 2\psi \\ +\frac{1}{4}J_p\dot\phi\sin\theta\sin 2\chi\sin 2\psi \\ +\frac{1}{2}J_t\dot\phi\cos^2\chi\cos^2\psi\sin 2\theta \end{array} \\
\begin{array}{c} -J_p\dot\theta\cos\psi \\ +2J_t\cos\psi\dot\theta \\ -2J_t\cos^2\theta\dot\theta\cos\psi \\ +2J_p\dot\theta\cos\psi\cos^2\theta \\ +\frac{1}{2}\dot\psi J_p\sin\psi\sin 2\theta\cos^2\chi \\ -\dot\psi J_p\cos\theta\sin\psi\sin\theta \\ +\frac{1}{2}\dot\psi J_p\sin\theta\cos\psi\sin 2\chi \\ -\frac{1}{2}\dot\psi J_t\sin\theta\cos\psi\sin 2\chi \\ -\frac{1}{2}\dot\psi J_t\cos^2\chi\sin\psi\sin 2\theta \\ +\frac{1}{2}\dot\psi J_t\sin 2\theta\sin\psi \\ -2J_t\cos^2\chi\dot\theta\cos\psi \\ +2J_p\cos^2\chi\cos\psi\dot\theta \\ -2J_p\dot\theta\cos\psi\cos^2\chi\cos^2\theta \\ +2J_t\cos^2\chi\cos^2\theta\cos\psi\dot\theta \end{array} &
\begin{array}{c} -2J_t\cos\theta\sin\theta\dot\theta \\ +2J_t\cos^2\chi\sin\theta\cos\theta\dot\theta \\ -2J_p\sin\theta\cos\theta\dot\theta\cos^2\chi \\ +2J_p\sin\theta\cos\theta\dot\theta \end{array} &
\begin{array}{c} J_t\cos\theta\dot\psi\sin\theta \\ -J_p\sin\theta\dot\psi\cos\theta \\ +J_p\sin\theta\dot\psi\cos\theta\cos^2\chi \\ -J_t\cos^2\chi\sin\theta\dot\psi\cos\theta \end{array} \\
\begin{array}{c} \frac{1}{2}\dot\theta J_t\sin\theta\cos\psi\sin 2\chi \\ -\frac{1}{2}\dot\theta J_p\sin\theta\cos\psi\sin 2\chi \end{array} &
\begin{array}{c} \dot\theta J_p\cos\chi\cos\theta\sin\chi \\ -\dot\theta J_t\cos\chi\cos\theta\sin\chi \end{array} & 0
\end{pmatrix}
\tag{A7}
$$

$$G^e_{11}(\Gamma_e) = \frac{G_u m_\oplus m_e}{\sqrt{x_e^2 + y_e^2 + z_e^2}} \begin{pmatrix} 1 & 0 & 0 \\ 0 & 1 & 0 \\ 0 & 0 & 1 \end{pmatrix} \tag{A9}$$

The matrices K_Γ, K_Φ, C_Γ, and C_Φ, which characterize the elastic reactions, take the form

$$K_\Gamma = \begin{pmatrix} k_t & 0 & 0 \\ 0 & k_t & 0 \\ 0 & 0 & k_t \end{pmatrix} \qquad K_\Phi = \begin{pmatrix} k_f & 0 & 0 \\ 0 & k_f & 0 \\ 0 & 0 & k_r \end{pmatrix} \tag{A10}$$

$$C_\Gamma = \begin{pmatrix} c_t & 0 & 0 \\ 0 & c_t & 0 \\ 0 & 0 & c_t \end{pmatrix} \qquad C_\Phi = \begin{pmatrix} c_f & 0 & 0 \\ 0 & c_f & 0 \\ 0 & 0 & c_r \end{pmatrix} \tag{A11}$$

The matrices $\mathcal{M}_i(\Phi_i)$, $\mathcal{M}_e(\Phi_e)$, $\mathcal{N}_i(\Phi_i)$, and $\mathcal{N}_e(\Phi_e)$ are

$$\mathcal{M}_i(\Phi_i) = \begin{pmatrix} 1 & 0 & 0 \\ 0 & 1 & 0 \\ \sin\psi_i & 0 & \cos\psi_i \end{pmatrix} \begin{pmatrix} 1 & 0 & 0 \\ 0 & \cos\phi_i & \sin\phi_i \\ 0 & -\sin\phi_i & \cos\phi_i \end{pmatrix} = \begin{pmatrix} 1 & 0 & 0 \\ 0 & \cos\phi_i & \sin\phi_i \\ \sin\psi_i & -\cos\psi_i \sin\phi_i & \cos\psi_i \cos\phi_i \end{pmatrix} \tag{A12}$$

$$\mathcal{M}_e(\Phi_e) = \begin{pmatrix} 1 & 0 & 0 \\ 0 & 1 & 0 \\ \sin\psi_e & 0 & \cos\psi_e \end{pmatrix} \begin{pmatrix} 1 & 0 & 0 \\ 0 & \cos\phi_e & \sin\phi_e \\ 0 & -\sin\phi_e & \cos\phi_e \end{pmatrix} = \begin{pmatrix} 1 & 0 & 0 \\ 0 & \cos\phi_e & \sin\phi_e \\ \sin\psi_e & -\cos\psi_e \sin\phi_e & \cos\psi_e \cos\phi_e \end{pmatrix} \tag{A13}$$

$$\mathcal{N}_i(\Phi_i) = \begin{pmatrix} \cos\psi_i & 0 & \sin\psi_i \\ 0 & 1 & 0 \\ 0 & 0 & 1 \end{pmatrix}$$

$$\mathcal{N}_e(\Phi_e) = \begin{pmatrix} \cos\psi_e & 0 & \sin\psi_e \\ 0 & 1 & 0 \\ 0 & 0 & 1 \end{pmatrix} \tag{A14}$$

The matrices E_i, E_e, U_i', U_i'', U_e, and U_d are

$$E_i = \begin{pmatrix} 0 & -\epsilon_{z_i} & \epsilon_{y_i} \\ \epsilon_{z_i} & 0 & -\epsilon_{x_i} \\ -\epsilon_{y_i} & \epsilon_{x_i} & 0 \end{pmatrix} \qquad E_e = \begin{pmatrix} 0 & -\epsilon_{z_e} & \epsilon_{y_e} \\ \epsilon_{z_e} & 0 & -\epsilon_{x_e} \\ -\epsilon_{y_e} & \epsilon_{x_e} & 0 \end{pmatrix} \tag{A15}$$

$$U_i' = \begin{pmatrix} 0 & -u'_{z_i} & u'_{y_i} \\ u'_{z_i} & 0 & -u'_{x_i} \\ -u'_{y_i} & u'_{x_i} & 0 \end{pmatrix} \qquad U_i'' = \begin{pmatrix} 0 & -u''_{z_i} & u''_{y_i} \\ u''_{z_i} & 0 & -u''_{x_i} \\ -u''_{y_i} & u''_{x_i} & 0 \end{pmatrix} \tag{A16}$$

$$U_e = \begin{pmatrix} 0 & -u_{z_e} & u_{y_e} \\ u_{z_e} & 0 & -u_{x_e} \\ -u_{y_e} & u_{x_e} & 0 \end{pmatrix} \qquad U_d = \begin{pmatrix} 0 & -u_{z_d} & u_{y_d} \\ u_{z_d} & 0 & -u_{x_d} \\ -u_{y_d} & u_{x_d} & 0 \end{pmatrix} \tag{A17}$$

Appendix B: Terms in Equations (31–33)

For the control model, described by Eqs. (31–33), B^i_{11} and B^e_{11} are the same of the simulation model, whereas $B^i_{22}(\Phi_i)$, $B^e_{22}(\Phi_e)$, $C^i_{22}(\Phi_i)$, and $C^e_{22}(\Phi_e)$ take the form

$$B^i_{22}(\Phi_i) = \begin{bmatrix} J_{t_i} & 0 & J_{p_i}\psi_i + \chi_i\left(J_{p_i} - J_{t_i}\right)\cos\theta_i \\ * & J_{t_i} & \chi_i\left(J_{p_i} - J_{t_i}\right)\sin\theta_i \\ * & * & J_{p_i} + J_{t_i}\chi_i^2 \end{bmatrix} \tag{B1}$$

$$B^e_{22}(\Phi_e) = \begin{bmatrix} J_{t_e} & 0 & J_{p_e}\psi_e + \chi_e\left(J_{p_e} - J_{t_e}\right)\cos\theta_e \\ * & J_{t_e} & \chi_e\left(J_{p_e} - J_{t_e}\right)\sin\theta_e \\ * & * & J_{p_e} + J_{t_e}\chi_e^2 \end{bmatrix} \tag{B2}$$

$$C^i_{22}(\Phi_i) = \begin{bmatrix} 0 & J_{p_i}\dot\theta_i & \chi_i\left(J_{t_i} - J_{p_i}\right)\dot\theta_i\sin\theta_i \\ -J_{p_i}\dot\theta_i & 0 & \chi_i\left(J_{p_i} - J_{t_i}\right)\dot\theta_i\cos\theta_i \\ J_{p_i}\dot\psi_i & 0 & 0 \end{bmatrix} \tag{B3}$$

$$C^e_{22}(\Phi_e) = \begin{bmatrix} 0 & J_{p_e}\dot\theta_e & \chi_e\left(J_{t_e} - J_{p_e}\right)\dot\theta_e\sin\theta_e \\ -J_{p_e}\dot\theta_e & 0 & \chi_e\left(J_{p_e} - J_{t_e}\right)\dot\theta_e\cos\theta_e \\ J_{p_e}\psi_e & 0 & 0 \end{bmatrix} \tag{B4}$$

$\Lambda_i, (\Phi_i)$ $\Lambda_e(\Phi_e)$, Σ_i, and Σ_e in Eqs. (31–33) take the form

$$\Lambda_i(\Phi_i) = \begin{bmatrix} 0 & \left(J_{p_i}/2J_{t_i}\right)\dot\theta_i & \left(J_{p_i}/2J_{t_i}\right)\dot\psi_i \\ -\left(J_{p_i}/2J_{t_i}\right)\dot\theta_i & 0 & -\left(J_{p_i}/2J_{t_i}\right)\dot\phi_i \\ 0 & 0 & 0 \end{bmatrix}$$

$$\Lambda_e(\Phi_e) = \begin{bmatrix} 0 & \left(J_{p_e}/2J_{t_e}\right)\dot\theta_e & \left(J_{p_e}/2J_{t_e}\right)\dot\psi_e \\ -\left(J_{p_e}/2J_{t_e}\right)\dot\theta_e & 0 & -\left(J_{p_e}/2J_{t_e}\right)\dot\phi_e \\ 0 & 0 & 0 \end{bmatrix} \tag{B5}$$

$$\Sigma_i = \begin{bmatrix} 1/J_{t_i} & 0 & 0 \\ 0 & 1/J_{t_i} & 0 \\ 0 & 0 & 1/\left(J_{p_i} + J_{t_i}\chi_i^2\right) \end{bmatrix}$$

$$\Sigma_e = \begin{bmatrix} 1/J_{t_e} & 0 & 0 \\ 0 & 1/J_{t_e} & 0 \\ 0 & 0 & 1/\left(J_{p_e} + J_{t_e}\chi_e^2\right) \end{bmatrix} \tag{B6}$$

Appendix C: Expression of Matrices $\mathcal{F}_i$ and $\mathcal{F}_e$

Matrices $\mathcal{F}_i(\tilde\Gamma_i)$ and $\mathcal{F}_e(\tilde\Gamma_e)$ in Eqs. (72) and (73) take the form

$$\frac{\mathcal{F}_i(\tilde\Gamma_i)}{G_u m_\oplus} = \frac{\begin{bmatrix} \begin{matrix}-2\tilde x_i^2 + \tilde y_i^2 \\ +z_i^2 + R^2\end{matrix} & -3\tilde x_i \tilde y_i & 3\tilde y_i\left(5\tilde x_i^2 - 1\right) & \frac{3}{2}\tilde x_i\left(5\tilde x_i^2 - 2\right) & \frac{15}{2}\tilde y_i^2 \tilde x_i \\ -3\tilde x_i \tilde y_i & \begin{matrix}-2\tilde y_i^2 + \tilde x_i^2 \\ +z_i^2 + R^2\end{matrix} & 3\tilde x_i\left(5\tilde y_i^2 - 1\right) & \frac{15}{2}\tilde x_i^2 \tilde y_i & \frac{3}{2}\tilde y_i\left(5\tilde y_i^2 - 2\right) \\ -3\tilde x_i z_i & -3\tilde y_i z_i & 15\tilde x_i \tilde y_i z_i & \frac{15}{2}\tilde x_i^2 z_i & \frac{15}{2}\tilde y_i^2 z_i \end{bmatrix}}{\left(\sqrt{\tilde x_i^2 + \tilde y_i^2 + z_i^2 + R^2}\right)^5} \tag{C1}$$

$$\frac{\mathcal{F}_e(\tilde{\Gamma}_e)}{G_u m_\oplus} = \frac{\begin{bmatrix} -2\tilde{x}_e^2+\tilde{y}_e^2+z_e^2+R^2 & -3\tilde{x}_e\tilde{y}_e & 3\tilde{y}_e\left(5\tilde{x}_e^2-1\right) & \frac{3}{2}\tilde{x}_e\left(5\tilde{x}_e^2-2\right) & \frac{15}{2}\tilde{y}_e^2\tilde{x}_e \\ -3\tilde{x}_e\tilde{y}_e & -2\tilde{y}_e^2+\tilde{x}_e^2+z_e^2+R^2 & 3\tilde{x}_e\left(5\tilde{y}_e^2-1\right) & \frac{15}{2}\tilde{x}_e^2\tilde{y}_e & \frac{3}{2}\tilde{y}_e\left(5\tilde{y}_e^2-2\right) \\ -3\tilde{x}_e z_e & -3\tilde{y}_e z_e & 15\tilde{x}_e\tilde{y}_e z_e & \frac{15}{2}\tilde{x}_e^2 z_e & \frac{15}{2}\tilde{y}_e^2 z_e \end{bmatrix}}{\left(\sqrt{\tilde{x}_e^2+\tilde{y}_e^2+z_e^2+R^2}\right)^5} \tag{C2}$$

Appendix D: Computations for Equations (109) and (110)

For the sake of computation, the rotational dynamics in Eqs. (31–33) has been simplified, yielding the linear form

$$\begin{pmatrix}\dot{\phi}_i\\ \dot{\psi}_i\\ \dot{\phi}_e\\ \dot{\psi}_e\\ \ddot{\phi}_i\\ \ddot{\psi}_i\\ \ddot{\phi}_e\\ \ddot{\psi}_e\end{pmatrix} = \begin{bmatrix} 0&0&0&0&1&0&0&0\\ 0&0&0&0&0&1&0&0\\ 0&0&0&0&0&0&1&0\\ 0&0&0&0&0&0&0&1\\ -k_f/J_{t_i} & 0 & k_f/J_{t_i} & 0 & -c_f/J_{t_i} & -\omega_s\left(J_{p_i}/J_{t_i}\right) & c_f/J_{t_i} & 0\\ 0 & -k_f/J_{t_i} & 0 & k_f/J_{t_i} & \omega_s\left(J_{p_i}/J_{t_i}\right) & -c_f/J_{t_i} & 0 & c_f/J_{t_i}\\ k_f/J_{t_e} & 0 & -k_f/J_{t_e} & 0 & c_f/J_{t_e} & 0 & -c_f/J_{t_e} & -\omega_s\left(J_{p_e}/J_{t_e}\right)\\ 0 & k_f/J_{t_e} & 0 & -k_f/J_{t_e} & 0 & c_f/J_{t_e} & \omega_s\left(J_{p_e}/J_{t_e}\right) & -c_f/J_{t_e} \end{bmatrix} \begin{pmatrix}\phi_i\\ \psi_i\\ \phi_e\\ \psi_e\\ \dot{\phi}_i\\ \dot{\psi}_i\\ \dot{\phi}_e\\ \dot{\psi}_e\end{pmatrix}$$
$$+ \begin{Bmatrix} 0 & -\chi_i\omega_s^2\left(J_{t_i}-J_{p_i}/J_{t_i}\right)\\ \chi_i\omega_s^2\left[\left(J_{t_i}-J_{p_i}\right)/J_{t_i}\right] & 0\\ 0 & -\chi_e\omega_s^2\left[\left(J_{t_e}-J_{p_e}\right)/J_{t_e}\right]\\ \chi_e\omega_s^2\left[\left(J_{t_e}-J_{p_e}\right)/J_{t_e}\right] & 0\\ 0&0\\ 0&0\\ 0&0\\ 0&0 \end{Bmatrix} \begin{pmatrix}\cos\omega_s t\\ \sin\omega_s t\end{pmatrix} \tag{D1}$$

The steady-state response of the rotational dynamics assumes the form

$$\phi_i = a_1\cos\omega_s t + b_1\sin\omega_s t \tag{D2}$$

$$\psi_i = a_2\cos\omega_s t + b_2\sin\omega_s t \tag{D3}$$

$$\theta_i = \omega_s t \tag{D4}$$

$$\phi_e = a_3\cos\omega_s t + b_3\sin\omega_s t \tag{D5}$$

$$\psi_e = a_4\cos\omega_s t + b_4\sin\omega_s t \tag{D6}$$

$$\theta_e = \omega_s t \tag{D7}$$

whose parameters a_i and b_i have been exactly computed; their expression is very complex, and so only the dependence on χ_i and χ_e is reported in Table D1 for the two earlier mentioned configurations, for example, for the TMs configuration $a_1 = 0.3612\times 10^{-4}\chi_i - 0.3612\times 10^{-4}\chi_e$ and so on. Therefore, it is immediate to conclude that, in first approximation, the steady-state solution is

$$\phi_i = \chi_i\cos\omega_s t \tag{D8}$$

$$\psi_i = -\chi_i\sin\omega_s t \tag{D9}$$

$$\theta_i = \omega_s t \tag{D10}$$

$$\phi_e = \chi_e\cos\omega_s t \tag{D11}$$

$$\psi_e = -\chi_e\sin\omega_s t \tag{D12}$$

$$\theta_e = \omega_s t \tag{D13}$$

finding the results of Eqs. (109) and (110).

References

[1]Isidori, A., *Nonlinear Control Systems*, 2nd ed., Springer-Verlag, London, 1989, Chap. 2.

[2]Nobili, A. M., Bramanti, D., Polacco, E., Catastini, G., Milani, A., Anselmo, L., Andrenucci, M., Marcuccio, S., Genta, G., Delprete, C., Brusa,

Table D1 Coefficients a_i and b_i computed for TMs and PGB–S/C configurations

Coefficient	χ_i (TM)	χ_e (TM)	χ_i (PGB–S/C)	χ_e (PGB–S/C)
a_1	0.3612×10^{-4}	-0.3612×10^{-4}	-0.2692×10^{-6}	0.2692×10^{-6}
b_1	1.003	-0.3588×10^{-2}	0.9999	0.2698×10^{-4}
a_2	−1.003	0.3588×10^{-2}	−0.9999	-0.2698×10^{-4}
b_2	0.3612×10^{-4}	-0.3612×10^{-4}	-0.2692×10^{-6}	0.2692×10^{-6}
a_3	-0.3612×10^{-4}	0.3612×10^{-4}	0.2816×10^{-7}	-0.2816×10^{-7}
b_3	-0.3588×10^{-2}	1.003	0.2822×10^{-5}	0.9999
a_4	0.3588×10^{-2}	−1.003	-0.2822×10^{-5}	−0.9999
b_4	-0.3612×10^{-4}	0.3612×10^{-4}	0.2816×10^{-7}	-0.281×10^{-7}

E., Bassani, D., Vannaroni, G., Dobrowolny, M., Melchioni, E., Arduini, C., Ponzi, U., Laneve, G., Mortari, D., Parisse, M., Curti, F., Cabiati, F., Rossi, E., Sosso, A., Zago, G., Monaco, S., Gori Giorgi, G., Battilotti, S., D'Antonio, L., and Amicucci, G., "'Galileo Galilei,' Flight Experiment on the Equivalence Principle with Field Emission Electric Propulsion," *Journal of Astronautical Sciences*, Vol. 43, No. 3, 1995, pp. 219–242.

[3]Nobili, A. M., Bramanti, D., Polacco, E., Mengali, G., Sebasta, A., Anselmi, A., Catastini, G., Portigliotti, S., Ancona, V., Bogo, W., Perachino, L., Di Gennaro, S., Lanza, P., Martella, P., Porta, P., Lenti, A., Ronchi, R., Isabella, L., Severi, A., Minucci, M., Fabri, G., Marcuccio, S., Monaco, S., Di Giamberardino, P., Ronchini, R., Genta, G., Brusa, E., Curti, F., Mortari, D., Cabiati, F., Comandi, G., Bardascino, M., Aversa, N., and Sabbatini, S., "Galileo Galilei (GG), A Small Satellite to Test the Equivalence Principle of Newton and Einstein," Agenzia Spaziale Italiana Phase A Rept., Nov. 1998.

[4]Nobili, A. M., Bramanti, D., Catastini, G., Anselmi, A., Portigliotti, S., Lenti, A., Volpi, G., and Marcuccio, S., "GALILEO GALILEI (GG)-Test of the Equivalence Principle with a Small Spinning Spacecraft: The Stabilization of Its Weakly Coupled Masses," *Scientific Satellites Achievements and Prospects in Europe*, Association Aéronatique et Astronatique de France-ESA Proceedings No. 3, 1996, pp. 74–89.

[5]Marcuccio, S., Genovese, A., and Andrenucci, M., "Experimental Performance of Field Emission Microthrusters," *Journal of Propulsion and Power*, Vol. 14, No. 5, 1998, pp. 774–781.

[6]Nobili, A. M., Bramanti, D., Polacco, E., Catastini, G., Anselmi, A., Portigliotti, S., Lenti, A., Di Giamberardino, P., Monaco, S., and Ronchini, R., "Evaluation of a Proposed Test of the Weak Equivalence Principle Using Earth-Orbiting Bodies in High-Speed Co-Rotation: Re-Establishing the Physical Bases," *Classical and Quantum Gravity*, Vol. 16, No. 4, 1999, pp. 1463–1470.

[7]Genta, G., *Vibration of Structures and Machines*, Springer-Verlag, New York, 1993, Chap. 2.

[8]Di Giamberardino, P., and Monaco, S., "On HALO Orbits Spacecraft Stabilization," *Acta Astronautica*, Vol. 38, No. 12, 1996, pp. 903–925.

[9]Gongfian, Y., and Xueyi, F., "Orbit Control for Low-Orbit Recoverable Satellite," *Intelligent Autonomous Control in Aerospace*, Pergamon, Oxford, England, U.K., 1997, pp. 175–178.

[10]Wertzt, J. R., "Implementing Autonomous Orbit Control," *Guidance and Control 1996*, Vol. 92, Advances in the Astronautical Sciences, American Astronautical Society, San Diego, CA, 1996, pp. 57–68.

[11]Jafry, Y., "Drag-Free Control for Ministep," *Classical and Quantum Gravity*, Vol. 13, No. 11A, 1996, pp. 179–184.

[12]Vinh, N. X., Johannesen, J. R., Mease, K. D., and Hanson, J. M., "Explicit Guidance of Drag-Modulated Aeroassisted Transfer Between Elliptical Orbits," *Journal of Guidance, Control, and Dynamics*, Vol. 9, No. 3, 1986, pp. 274–280.

[13]Vaillon, L., Borde, J., Duhamel, T., and Damilano, P., "Drag-Free Control Systems and Technologies," *Space Technology*, Vol. 16, No. 5-6, 1996, pp. 245–254.